Spatio-Temporal Analysis of Epidemic Phenomena Using the **R** Package **surveillance**

Sebastian Meyer
University of Zurich

Leonhard Held
University of Zurich

Michael Höhle
Stockholm University

Abstract

The availability of geocoded health data and the inherent temporal structure of communicable diseases have led to an increased interest in statistical models and software for spatio-temporal data with epidemic features. The open source R package **surveillance** can handle various levels of aggregation at which infective events have been recorded: individual-level time-stamped geo-referenced data (case reports) in either continuous space or discrete space, as well as counts aggregated by period and region. For each of these data types, the **surveillance** package implements tools for visualization, likelihoood inference and simulation from recently developed statistical regression frameworks capturing endemic and epidemic dynamics. Altogether, this paper is a guide to the spatio-temporal modeling of epidemic phenomena, exemplified by analyses of public health surveillance data on measles and invasive meningococcal disease.

1. Introduction

Epidemic data are realizations of spatio-temporal processes with autoregressive or "self-exciting" behavior. Examples of epidemic phenomena beyond infectious diseases include earth quakes (Ogata 1999), crimes (Johnson 2010; Mohler, Short, Brantingham, Schoenberg, and Tita 2011), invasive species (Balderama, Schoenberg, Murray, and Rundel 2012), and forest fires (Vrbik, Deardon, Feng, Gardner, and Braun 2012). Epidemic data are special with regard to at least three aspects, which hinder the application of classical statistical approaches: the data are rarely a result of planned experiments, the observations (cases, events) are not independent, and often the process is only partially observable.

Since 2005, the open source R (R Core Team 2015) package **surveillance** provides a growing computational framework for methodological developments and practical tools for the *monitoring* and *modeling* of epidemic phenomena – traditionally in the context of infectious diseases. Monitoring is concerned with prospective aberration detection for which several algorithms have been implemented as described by Höhle (2007) and recently updated and reviewed by Salmon, Schumacher, and Höhle (2015). The other major purpose of the **surveillance** package and the focus of this paper is the regression-oriented modeling of spatio-temporal epidemic data. This enables the user to a) assess the role of environmental factors, socio-demographic characteristics, or control measures in shaping endemic and epidemic dynamics, b) analyze the spatio-temporal interaction of events, and c) simulate the epidemic spread from estimated models.

The implemented statistical modeling frameworks have already been successfully applied to a broad range of surveillance data, e.g., human influenza (Paul, Held, and Toschke 2008; Paul and Held 2011; Geilhufe, Held, Skrøvseth, Simonsen, and Godtliebsen 2014), meningococcal disease (Paul *et al.* 2008; Paul and Held 2011; Meyer, Elias, and Höhle 2012), measles (Herzog, Paul, and Held 2011), psychiatric hospital admissions (Meyer, Warnke, Rössler, and Held 2015), rabies in foxes (Höhle, Paul, and Held 2009), coxiellosis in cows (Schrödle, Held, and Rue 2012), and the classical swine fever virus (Höhle 2009). Although these applications all originate from public or animal health surveillance, we stress that our methods also apply to the other epidemic phenomena described above.

To the best of our knowledge, no other software can estimate regression models for spatio-temporal epidemic data. There are, however, some related R packages that we like to mention here, since they also deal with epidemic phenomena. For instance, the *R-epi project*[1] lists the package **EpiEstim** (Cori, Ferguson, Fraser, and Cauchemez 2013), which can estimate the average number of secondary cases caused by an infected individual, the so-called reproduction number, from a time series of disease incidence. Similar functionality is provided by the package **R0** (Obadia, Haneef, and Boelle 2012). Other packages are designed to estimate transmission characteristics from phylogenetic trees (**TreePar**, Stadler and Bonhoeffer 2013), or to reconstruct transmission trees from sequence data (**outbreaker**, Jombart, Cori, Didelot, Cauchemez, Fraser, and Ferguson 2014). The package **amei** (Merl, Johnson, Gramacy, and Mangel 2010) is targeted towards finding optimal intervention strategies, e.g., the proportion of the population to be vaccinated to prevent further disease spread, using purely temporal epidemic models. The recently published package **tscount** (Liboschik, Fokianos, and Fried 2015) is dedicated to the analysis of count time series with serial correlation such as the number of stock market transitions per minute or the weekly number of reported infections of a particular disease. The **tscount** package can fit a univariate version of the areal count time-series model presented in Section 5. For a purely spatial analysis of disease occurrence, see, e.g., the recent paper by Brown (2015) introducing the package **diseasemapping**. One of the few packages fitting spatio-temporal epidemic models is **etasFLP** (Adelfio and Chiodi 2015). The Epidemic-Type Aftershock-Sequences (ETAS) model for earthquakes (Ogata 1999) is closely related to the endemic-epidemic point process model described in Section 3, but incorporates seismological laws rather than covariates. The long-standing package **splancs** (Rowlingson and Diggle 2015) offers diagnostic tools to investigate space-time clustering in a point pattern, i.e., to check if the process at hand shows self-exciting epidemic behavior. Statistical tests for space-time interaction are discussed in Meyer *et al.* (2015), who propose

---

[1] https://sites.google.com/site/therepiproject/

a test based on the regression framework of Section 3. An important recent development for spatio-temporal tasks in R are the basic data classes and utility functions provided by the dedicated package **spacetime** (Pebesma 2012), which builds upon the quasi standards **sp** (Bivand, Pebesma, and Gómez-Rubio 2013) for spatial data and **xts** (Ryan and Ulrich 2014) for time-indexed data, respectively. For a more general overview of R packages for spatio-temporal data, see the CRAN Task View "Handling and Analyzing Spatio-Temporal Data" (Pebesma 2015). A non-R option is the *Spatiotemporal Epidemiological Modeler* (STEM) tool[2]. It has a graphical user interface and can simulate the evolution of disease incidence in a population. The ability to estimate model parameters from surveillance data, however, is limited to simple non-spatial models. WinBUGS has been used for Bayesian inference of specialized spatio-temporal epidemic models (Malesios, Demiris, Kalogeropoulos, and Ntzoufras 2014).

The remainder of this paper is organized as follows: Section 2 gives a brief overview of the three statistical models for spatio-temporal epidemic data implemented in **surveillance**. Each of the subsequent model-specific Sections 3 to 5 first describes the associated methodology and then illustrates the model implementation – including data handling, visualization, inference, and simulation – by applications to infectious disease surveillance data. Section 6 concludes the paper.

2. Spatio-temporal endemic-epidemic modeling

Epidemic models traditionally describe the spread of a communicable disease in a population. Often, a compartmental view of the population is taken, placing individuals into one of the three states (S)usceptible, (I)nfectious, or (R)emoved. Modeling the transitions between these states in a closed population using deterministic differential equations dates back to the work of Kermack and McKendrick (1927). Considering a stochastic version of the simplest homogeneous SIR model in a closed population of size N, the hazard rate for a susceptible individual $i \in S(t)$ to become infectious at time t – the so-called force of infection – is

$$\lambda_i(t) = \sum_{j \in I(t)} \beta \,. \tag{1}$$

Here, $S(t), I(t) \subseteq \{1, \ldots, N\}$ denote the index sets of currently susceptible and infectious individuals, respectively, and the parameter $\beta > 0$ is called the transmission rate. The stochastic SIR model is complemented by a distributional assumption about how long individuals are infective, where typical choices are the exponential or the gamma distribution. The set of recovered individuals at time t is found as $R(t) = \{1, \ldots, N\} \setminus (S(t) \cup I(t))$. The above homogeneous SIR model has since been extended in a multitude of ways, e.g., by additional states (addressing population heterogeneities arising from age groups, spatial location or vaccination) or population demographics. Overviews of SIR modeling approaches can be found in Anderson and May (1991), Daley and Gani (1999), and Keeling and Rohani (2008). The estimation of SIR model parameters from actual observed data is, however, often only treated marginally in such descriptions. In contrast, a number of more statistically flavored epidemic models have emerged recently. This includes, e.g., the TSIR model (Finkenstädt and Grenfell 2000), two-component time-series models (Held, Höhle, and Hofmann 2005; Held, Hofmann,

---

[2] https://www.eclipse.org/stem/

Höhle, and Schmid 2006), and point process models (Lawson and Leimich 2000; Diggle 2006). An overview of temporal and spatio-temporal epidemic models and their relation to the underlying metapopulation SIR models can be found in Höhle (2016).

At the heart of any statistical analysis is the subject-matter scientific problem, which a data-driven analysis seeks to address. Due to the generality and complexity of such problems we adopt here a technocratic view and let the available data guide what a "useful" epidemic model is. The **surveillance** package offers regression-oriented modeling frameworks for three different types of spatio-temporal data distinguished by the spatial and temporal resolution (Table 1). First, if an entire region is continuously monitored for infective events, which are time-stamped, geo-referenced, and potentially enriched with further event-specific data, then a (marked) spatio-temporal point pattern arises. Such continuous space-time epidemic data can be viewed as a realization of a self-exciting spatio-temporal point process (Section 3). The second data type we consider comprises the event history of a discrete set of units followed over time – e.g., farms during livestock epidemics – while registering when they become susceptible, infected, and potentially removed (neither at risk nor infectious). These data fit into the framework of a spatial SIR model represented as a multivariate temporal point process (Section 4). Our third data type is often encountered as a result of privacy protection or reporting regimes, and is an aggregated version of the individual event data mentioned first: event counts by region and period. Such areal count time series can be fitted with the multivariate negative binomial time-series model presented in Section 5.

The three aforementioned model classes are all inspired by the Poisson branching process with immigration approach proposed by Held *et al.* (2005). Its main characteristic is the additive decomposition of disease risk into *endemic* and *epidemic* features, similar to the *background* and *triggered* components in the ETAS model for earthquake occurrence. The endemic component describes the risk of new events by external factors independent of the history of the epidemic process. In the context of infectious diseases, such factors may include seasonality, population density, socio-demographic variables, and vaccination coverage – all potentially varying in time and/or space. Explicit dependence between events is then introduced through an epidemic component driven by the observed past.

Each of the following three model-specific sections starts with a brief theoretical introduction to the respective spatio-temporal endemic-epidemic model, before we describe the implementation using the example data mentioned in Table 1.

	twinstim (Section 3)	twinSIR (Section 4)	hhh4 (Section 5)
Data class	epidataCS	epidata	sts
Resolution	individual events in continuous space-time	individual SI[R][S] event history of a fixed population	event counts aggregated by region and time period
Example	cases of meningococcal disease, Germany, 2002–8	measles outbreak among children in Hagelloch, 1861	weekly counts of measles by district, Weser-Ems, 2001–2
Model	(marked) spatio-temporal point process	multivariate temporal point process	multivariate time series (Poisson or NegBin)
Reference	Meyer *et al.* (2012)	Höhle (2009)	Held and Paul (2012)

Table 1: Spatio-temporal endemic-epidemic models and corresponding data classes implemented in the R package **surveillance**.

3. Spatio-temporal point pattern of infective events

The endemic-epidemic spatio-temporal point process model "`twinstim`" is designed for point-referenced, individual-level surveillance data. As an illustrative example, we use case reports of invasive meningococcal disease (IMD) caused by the two most common bacterial finetypes of meningococci in Germany, 2002–2008, as previously analyzed by Meyer *et al.* (2012) and Meyer and Held (2014a). We start by describing the general model class in Section 3.1. Section 3.2 introduces the example data and the associated class `epidataCS`, Section 3.3 presents the core functionality of fitting and analyzing such data using `twinstim`, and Section 3.4 shows how to simulate realizations from a fitted model.

3.1. Model class: `twinstim`

Infective events occur at specific points in continuous space and time, which gives rise to a spatio-temporal point pattern $\{(\boldsymbol{s}_i, t_i) : i = 1, \ldots, n\}$ from a region $\boldsymbol{W}$ observed during a period $(0, T]$. The locations $\boldsymbol{s}_i$ and time points t_i of the n events can be regarded as a realization of a self-exciting spatio-temporal point process, which can be characterized by its conditional intensity function (CIF, also termed intensity process) $\lambda(\boldsymbol{s}, t)$. It represents the instantaneous event rate at location $\boldsymbol{s}$ at time point t given all past events, and is often more verbosely denoted by λ^* or by explicit conditioning on the "history" $\mathcal{H}_t$ of the process. Daley and Vere-Jones (2003, Chapter 7) provide a rigorous mathematical definition of this concept, which is key to likelihood analysis and simulation of "evolutionary" point processes.

Meyer *et al.* (2012) formulated the model class "`twinstim`" – a *two*-component *spatio-temporal intensity model* – by a superposition of an endemic and an epidemic component:

$$\lambda(\boldsymbol{s}, t) = \nu_{[\boldsymbol{s}][t]} + \sum_{j \in I(\boldsymbol{s}, t)} \eta_j \, f(\|\boldsymbol{s} - \boldsymbol{s}_j\|) \, g(t - t_j) \,. \tag{2}$$

This model constitutes a branching process with immigration, where part of the event rate is due to the first, endemic component, which reflects sporadic events caused by unobserved sources of infection. This background rate of new events is modelled by a piecewise constant log-linear predictor $\nu_{[\boldsymbol{s}][t]}$ incorporating regional and/or time-varying characteristics. Here, the space-time index $[\boldsymbol{s}][t]$ refers to the region covering $\boldsymbol{s}$ during the period containing t and thus spans a whole spatio-temporal grid on which the involved covariates are measured, e.g., district × month. We will later see that the endemic component therefore simply equals an inhomogeneous Poisson process for the event counts by cell of that grid.

The second, observation-driven epidemic component adds "infection pressure" from the set

$$I(\boldsymbol{s}, t) = \left\{ j : t_j < t \, \wedge \, t - t_j \leq \tau_j \, \wedge \, \|\boldsymbol{s} - \boldsymbol{s}_j\| \leq \delta_j \right\}$$

of past events and hence makes the process "self-exciting". During its infectious period of length τ_j and within its spatial interaction radius δ_j, the model assumes each event j to trigger further events, which are called offspring, secondary cases, or aftershocks, depending on the application. The triggering rate (or force of infection) is proportional to a log-linear predictor η_j associated with event-specific characteristics ("marks") $\boldsymbol{m}_j$, which are usually attached to the point pattern of events. The decay of infection pressure with increasing spatial and temporal distance from the infective event is modelled by parametric interaction functions f and g, respectively (Lawson and Leimich 2000, Section 4). A simple assumption

for the time course of infectivity is $g(t) = 1$. Alternatives include exponential decay, a step function, or empirically derived functions such as Omori's law for aftershock intervals (Utsu, Ogata, and Matsu'ura 1995). With regard to spatial interaction, the statistician's standard choice is a Gaussian kernel $f(x) = \exp\{-x^2/(2\sigma^2)\}$. However, in modeling the spread of human infectious diseases on larger scales, a heavy-tailed power-law kernel $f(x) = (x + \sigma)^{-d}$ was found to perform better (Meyer and Held 2014a). The (possibly infinite) upper bounds τ_j and δ_j provide a way of modeling event-specific interaction ranges. However, since these need to be pre-specified, a common assumption is $\tau_j \equiv \tau$ and $\delta_j \equiv \delta$, where the infectious period τ and the spatial interaction radius δ are determined by subject-matter considerations.

Model-based effective reproduction numbers

Similar to the simple SIR model (see, e.g., Keeling and Rohani 2008, Section 2.1), the above point process model (2) features a reproduction number derived from its branching process interpretation. As soon as an event occurs (individual becomes infected), it triggers offspring (secondary cases) around its origin $(\boldsymbol{s_j}, t_j)$ according to an inhomogeneous Poisson process with rate $\eta_j\, f(\|\boldsymbol{s} - \boldsymbol{s_j}\|)\, g(t - t_j)$. Since this triggering process is independent of the event's parentage and of other events, the expected number μ_j of events triggered by event j can be obtained by integrating the triggering rate over the observed interaction domain:

$$\mu_j = \eta_j \cdot \left[\int_0^{\min(T-t_j, \tau_j)} g(t)\, dt \right] \cdot \left[\int_{\boldsymbol{R_j}} f(\|\boldsymbol{s}\|)\, d\boldsymbol{s} \right] , \tag{3}$$

where

$$\boldsymbol{R_j} = (b(\boldsymbol{s_j}, \delta_j) \cap \boldsymbol{W}) - \boldsymbol{s_j} \tag{4}$$

is event j's influence region centered at $\boldsymbol{s_j}$, and $b(\boldsymbol{s_j}, \delta_j)$ denotes the disc centered at $\boldsymbol{s_j}$ with radius δ_j. Note that the above model-based reproduction number μ_j is event-specific since it depends on event marks through η_j, on the ranges of interaction δ_j and τ_j, as well as on the event location $\boldsymbol{s_j}$ and time point t_j.

Equation 3 can also be motivated by looking at a spatio-temporal version of the simple SIR model (1) wrapped into the `twinstim` class (2). This means: no endemic component, homogeneous force of infection ($\eta_j \equiv \beta$), homogeneous mixing in space ($f(x) = 1$, $\delta_j \equiv \infty$), and exponential decay of infectivity ($g(t) = e^{-\alpha t}$, $\tau_j \equiv \infty$). Then, for $T \to \infty$,

$$\mu = \beta \cdot \left[\int_0^\infty e^{-\alpha t}\, dt \right] \cdot \left[\int_{\boldsymbol{W} - \boldsymbol{s_j}} 1\, d\boldsymbol{s} \right] = \beta \cdot |\boldsymbol{W}|/\alpha ,$$

which corresponds to the basic reproduction number known from the simple SIR model by interpreting $|\boldsymbol{W}|$ as the population size, β as the transmission rate and α as the removal rate. Like in classic epidemic models, the process is sub-critical if $\mu < 1$ holds, which means that its eventual extinction is almost sure.

However, it is crucial to understand that in a full model with an endemic component, new infections may always occur via "immigration". Hence, reproduction numbers in `twinstim` are adjusted for infections occurring independently of previous infections. This also means that a misspecified endemic component may distort model-based reproduction numbers (Meyer *et al.* 2015). Furthermore, under-reporting and implemented control measures imply that the estimates are to be thought of as *effective* reproduction numbers.

Likelihood inference

The log-likelihood of the point process model (2) is a function of all parameters in the log-linear predictors $\nu_{[\boldsymbol{s}][t]}$ and η_j and in the interaction functions f and g. It has the form

$$\left[\sum_{i=1}^{n} \log \lambda(\boldsymbol{s}_i, t_i)\right] - \int_0^T \int_{\boldsymbol{W}} \lambda(\boldsymbol{s}, t)\, \mathrm{d}\boldsymbol{s}\, \mathrm{d}t\,. \tag{5}$$

To estimate the model parameters, we maximize the above log-likelihood numerically using the quasi-Newton algorithm available through the R function `nlminb`. We thereby make use of the analytical score function and an approximation of the expected Fisher information worked out by Meyer *et al.* (2012, Web Appendices A and B).

The space-time integral in the log-likelihood poses no difficulties for the endemic component of $\lambda(\boldsymbol{s}, t)$ since it is piecewise constant. However, integration of the epidemic component has a clear computational bottleneck: two-dimensional integrals $\int_{\boldsymbol{R}_i} f(\|\boldsymbol{s}\|)\, \mathrm{d}\boldsymbol{s}$ over the influence regions $\boldsymbol{R}_i$ of Equation 4, which are computationally represented by polygons (as is $\boldsymbol{W}$). Similar integrals appear in the score function, where $f(\|\boldsymbol{s}\|)$ is replaced by partial derivatives with respect to kernel parameters, e.g., $\partial f(\|\boldsymbol{s}\|)/\partial \log \sigma$ for the Gaussian kernel with standard deviation estimated on the log-scale. Calculation of these integrals is trivial for (piecewise) constant f, but otherwise requires numerical integration. For this purpose, the R package **polyCub** (Meyer 2015) offers cubature methods for polygonal domains as described in Meyer and Held (2014b, Section 2). For Gaussian f, we apply the two-dimensional midpoint rule with a σ-adaptive bandwidth, combined with an analytical formula via the χ^2 distribution if the 6σ-circle around $\boldsymbol{s}_i$ is contained in $\boldsymbol{R}_i$ (Meyer *et al.* 2012). The integrals in the score function are approximated by product Gauss cubature (Sommariva and Vianello 2007). For the recently implemented power-law kernels (Meyer and Held 2014a), we apply a particularly appealing method which takes analytical advantage of the assumed isotropy of spatial interaction in such a way that numerical integration remains in only one dimension (Meyer and Held 2014b, Section 2.4). As a general means to reduce the computational burden during numerical log-likelihood maximization, we **memoise** (Wickham 2014) the cubature function, which avoids redundant re-evaluations of the integral with identical parameters of f.

Special case: Endemic-only `twinstim`

As mentioned above, a `twinstim` model *without* an epidemic component can actually be represented as a Poisson regression model for aggregated counts. This provides a nice link to ecological regression approaches in general (Waller and Gotway 2004) and to the count data model `hhh4` illustrated in Section 5. To see this, recall that the endemic component $\nu_{[\boldsymbol{s}][t]}$ of a `twinstim` (2) is piecewise constant on the spatio-temporal grid with cells $([\boldsymbol{s}], [t])$. Hence the log-likelihood (5) of an endemic-only `twinstim` simplifies to a sum over all these cells,

$$\sum_{[\boldsymbol{s}],[t]} \left\{ Y_{[\boldsymbol{s}][t]} \log \nu_{[\boldsymbol{s}][t]} - |[\boldsymbol{s}]|\, |[t]|\, \nu_{[\boldsymbol{s}][t]} \right\}\,,$$

where $Y_{[\boldsymbol{s}][t]}$ is the aggregated number of events observed in cell $([\boldsymbol{s}], [t])$, and $|[\boldsymbol{s}]|$ and $|[t]|$ denote cell area and length, respectively. Except for an additive constant, the above log-likelihood is equivalently obtained from the Poisson model $Y_{[\boldsymbol{s}][t]} \sim \mathrm{Po}(|[\boldsymbol{s}]|\, |[t]|\, \nu_{[\boldsymbol{s}][t]})$. This relation offers a means of code validation using the established `glm` function to fit an endemic-only `twinstim` model, see the examples in `help("glm_epidataCS")`.

Extension: `twinstim` *with event types*

To model the example data on invasive meningococcal disease in the remainder of this section, we actually need to use an extended version $\lambda(\boldsymbol{s}, t, k)$ of Equation 2, which accounts for different event types k with own transmission dynamics. This introduces a further dimension in the point process, and the second log-likelihood component in Equation 5 accordingly splits into a sum over all event types. We refer to Meyer *et al.* (2012, Sections 2.4 and 3) for the technical details of this type-specific `twinstim` class. The basic idea is that the meningococcal finetypes share the same endemic pattern (e.g., seasonality), while infections of different finetypes are not associated via transmission. This means that the force of infection is restricted to previously infected individuals with the same bacterial finetype k, i.e., the epidemic sum in Equation 2 is over the set $I(\boldsymbol{s}, t, k) = I(\boldsymbol{s}, t) \cap \{j : k_j = k\}$. The implementation has limited support for type-dependent interaction functions f_{k_j} and g_{k_j} (not further considered here).

3.2. Data structure: `epidataCS`

The first step toward fitting a `twinstim` is to turn the relevant data into an object of the dedicated class `epidataCS`.[3] The primary ingredients of this class are a spatio-temporal point pattern (`events`) and its underlying observation region (`W`). An additional spatio-temporal grid (`stgrid`) holds (time-varying) areal-level covariates for the endemic regression part. We exemplify this data class by the `epidataCS` object for the 636 cases of invasive meningococcal disease in Germany originally analyzed by Meyer *et al.* (2012). It is already contained in the **surveillance** package as `data("imdepi")` and has been constructed as follows:

```
R> imdepi <- as.epidataCS(events = events, W = stateD, stgrid = stgrid,
+    qmatrix = diag(2), nCircle2Poly = 16)
```

The function `as.epidataCS` checks the consistency of the three data ingredients described in detail below. It also pre-computes auxiliary variables for model fitting, e.g., the individual influence regions (4), which are intersections of the observation region with discs approximated by polygons with `nCircle2Poly = 16` edges. The intersections are computed using functionality of the package **polyclip** (Johnson 2015). For multitype epidemics as in our example, the additional indicator matrix `qmatrix` specifies transmissibility across event types. An identity matrix corresponds to an independent spread of the event types, i.e., cases of one type can not produce cases of another type.

Data ingredients

The core `events` data must be provided in the form of a `SpatialPointsDataFrame` as defined by the package **sp** (Bivand *et al.* 2013):

```
R> summary(events)

Object of class SpatialPointsDataFrame
Coordinates:
    min  max
x 4039 4665
y 2710 3525
```

---

[3] The suffix "CS" indicates that the data-generating point process is indexed in continuous space.

```
Is projected: TRUE
proj4string :
[+init=epsg:3035 +units=km +proj=laea +lat_0=52 +lon_0=10 +x_0=4321000 +y_0=3210000
+ellps=GRS80 +no_defs]
Number of points: 636
Data attributes:
     time           tile      type      eps.t        eps.s          sex         agegrp
Min.   :   0   05354  : 34   B:336   Min.   :30   Min.   :200   female:292   [0,3)  :194
1st Qu.: 539   05370  : 27   C:300   1st Qu.:30   1st Qu.:200   male  :339   [3,19) :279
Median :1155   11000  : 27           Median :30   Median :200   NA's  :  5   [19,Inf):162
Mean   :1193   05358  : 13           Mean   :30   Mean   :200                NA's   :  1
3rd Qu.:1808   05162  : 12           3rd Qu.:30   3rd Qu.:200
Max.   :2543   05382  : 12           Max.   :30   Max.   :200
               (Other):511
```

The associated event coordinates are residence postcode centroids, projected in the *European Terrestrial Reference System 1989* (in kilometer units) to enable Euclidean geometry. See the `spTransform`-methods in package **rgdal** (Bivand, Keitt, and Rowlingson 2015) for how to project latitude and longitude coordinates into a planar coordinate reference system (CRS). The data frame associated with these spatial coordinates ($\boldsymbol{s}_i$) contains a number of required variables and additional event marks (in the notation of Section 3.1: $\{(t_i, [\boldsymbol{s}_i], k_i, \tau_i, \delta_i, \boldsymbol{m}_i) : i = 1, \ldots, n\}$). For the IMD data, the event `time` is measured in days since the beginning of the observation period 2002–2008 and is subject to a tie-breaking procedure (described later). The `tile` column refers to the region of the spatio-temporal grid where the event occurred and here contains the official key of the administrative district of the patient's residence. There are two `type`s of events labeled as `"B"` and `"C"`, which refer to the serogroups of the two meningococcal finetypes *B:P1.7-2,4:F1-5* and *C:P1.5,2:F3-3* contained in the data. The `eps.t` and `eps.s` columns specify upper limits for temporal and spatial interaction, respectively. Here, the infectious period is assumed to last a maximum of 30 days and spatial interaction is limited to a 200 km radius for all cases. The latter has numerical advantages for a Gaussian interaction function f with a relatively small standard deviation. For a power-law kernel, however, this restriction will be dropped to enable occasional long-range transmission. The last two data attributes displayed in the above `event` summary are covariates from the case reports: the gender and age group of the patient.

For the observation region `W`, we use a polygon representation of Germany's boundary. Since the observation region defines the integration domain in the point process log-likelihood (5), the more detailed the polygons of `W` are the longer it will take to fit a `twinstim`. It is thus advisable to sacrifice some shape details for speed by reducing the polygon complexity, e.g., by applying one of the simplification methods available at MapShaper.org (Harrower and Bloch 2006). Alternative tools in R are **spatstat**'s `simplify.owin` procedure (Baddeley, Rubak, and Turner 2015) and the function `thinnedSpatialPoly` in package **maptools** (Bivand and Lewin-Koh 2015), which implements the Douglas and Peucker (1973) reduction method. The **surveillance** package already contains a simplified representation of Germany's boundaries:

```
R> load(system.file("shapes", "districtsD.RData", package = "surveillance"))
```

This file contains both the `SpatialPolygonsDataFrame districtsD` of Germany's 413 administrative districts as at January 1, 2009, as well as their union `stateD`. These boundaries are projected in the same CRS as the `events` data.

The `stgrid` input specific to the endemic model component is a simple data frame with (time-dependent) areal-level covariates, e.g., socio-economic or ecological characteristics. For our IMD example, we have:

```
      start stop  tile   area popdensity
1         0   31 01001   56.4     1557.1
2         0   31 01002  118.7     1996.6
3         0   31 01003  214.2      987.6
...     ...  ...   ...    ...        ...
34690  2526 2557 16075 1148.5       79.2
34691  2526 2557 16076  843.5      133.6
34692  2526 2557 16077  569.1      181.5
```

Numeric (`start`,`stop`] columns index the time periods and the factor variable `tile` identifies the regions of the grid. Note that the given time intervals (here: months) also define the resolution of possible time trends and seasonality of the piecewise constant endemic intensity. We choose monthly intervals to reduce package size and computational cost compared to the weekly resolution originally used by Meyer *et al.* (2012) and Meyer and Held (2014a). The above `stgrid` data frame thus consists of 7 (years) times 12 (months) blocks of 413 (districts) rows each. The `area` column gives the area of the respective `tile` in square kilometers (compatible with the CRS used for `events` and `W`). A geographic representation of the regions in `stgrid` is not required for model estimation, and is thus not part of the `epidataCS` class. In our example, the areal-level data only consists of the population density `popdensity`, whereas Meyer *et al.* (2012) additionally incorporated (lagged) weekly influenza counts by district as a time-dependent covariate.

Data handling and visualization

The generated `epidataCS` object `imdepi` is a simple list of the checked ingredients `events`, `stgrid`, `W` and `qmatrix`. Several methods for data handling and visualization are available for such objects as listed in Table 2 and briefly presented in the remainder of this section.

Printing an `epidataCS` object presents some metadata and the first 6 events by default:

```
R> imdepi


Observation period: 0 – 2557
Observation window (bounding box): [4031, 4672] x [2684, 3550]
Spatio-temporal grid (not shown): 84 time blocks x 413 tiles
Types of events: "B" "C"
Overall number of events: 636

   coordinates   time  tile type eps.t eps.s    sex   agegrp BLOCK start popdensity
1 (4110, 3200)  0.212 05554    B    30   200   male   [3,19)     1     0        261
2 (4120, 3080)  0.712 05382    C    30   200   male   [3,19)     1     0        519
3 (4410, 2920)  5.591 09574    B    30   200 female [19,Inf)     1     0        209
4 (4200, 2880)  7.117 08212    B    30   200 female   [3,19)     1     0       1666
5 (4130, 3220) 22.060 05554    C    30   200   male   [3,19)     1     0        261
6 (4090, 3180) 24.954 05170    C    30   200   male   [3,19)     1     0        455
[....]
```

During conversion to `epidataCS`, the last three columns `BLOCK` (time interval index), `start` and `popdensity` have been merged from the checked `stgrid` to the `events` data frame. The event marks including time and location can be extracted in a standard data frame by `marks(imdepi)`, and this is summarized by `summary(imdepi)`.

Display	Subset	Extract	Modify	Convert
print	[	nobs	update	as.epidata
summary	head	marks	untie	*epidataCS2sts*
plot	tail			
animate	subset			
as.stepfun				

Table 2: Generic and *non-generic* functions applicable to `epidataCS` objects.

A simple plot of the number of infectives as a function of time (Figure 1) can be obtained by the step function converter:

```
R> plot(as.stepfun(imdepi), xlim = summary(imdepi)$timeRange, xaxs = "i",
+    xlab = "Time [days]", ylab = "Current number of infectives", main = "")
```
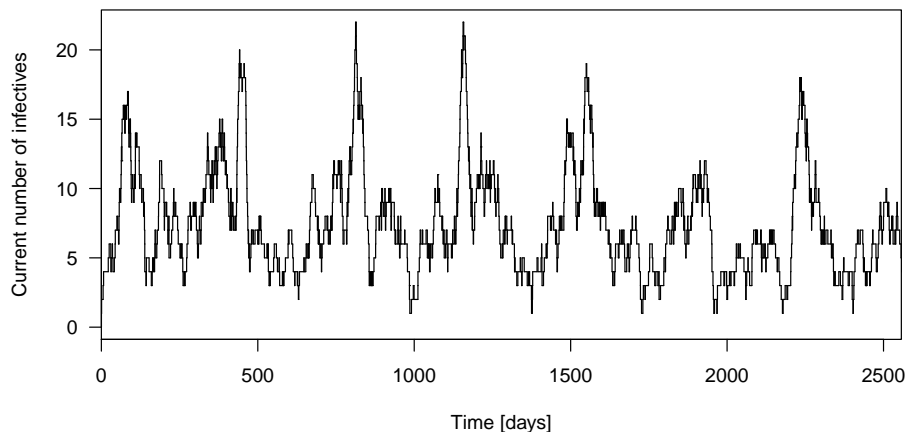

Figure 1: Time course of the number of infectives assuming infectious periods of 30 days.

The `plot`-method for `epidataCS` offers aggregation of the events over time or space:

```
R> plot(imdepi, "time", col = c("indianred", "darkblue"), ylim = c(0, 20))
R> plot(imdepi, "space", lwd = 2,
+    points.args = list(pch = c(1, 19), col = c("indianred", "darkblue")))
R> layout.scalebar(imdepi$W, scale = 100, labels = c("0", "100 km"), plot = TRUE)
```

The time-series plot (Figure 2a) shows the monthly aggregated number of cases by finetype in a stacked histogram as well as each type's cumulative number over time. The spatial plot (Figure 2b) shows the observation window `W` with the locations of all cases (by type), where the areas of the points are proportional to the number of cases at the respective location. Additional shading by the population is possible and exemplified in `help("plot.epidataCS")`.
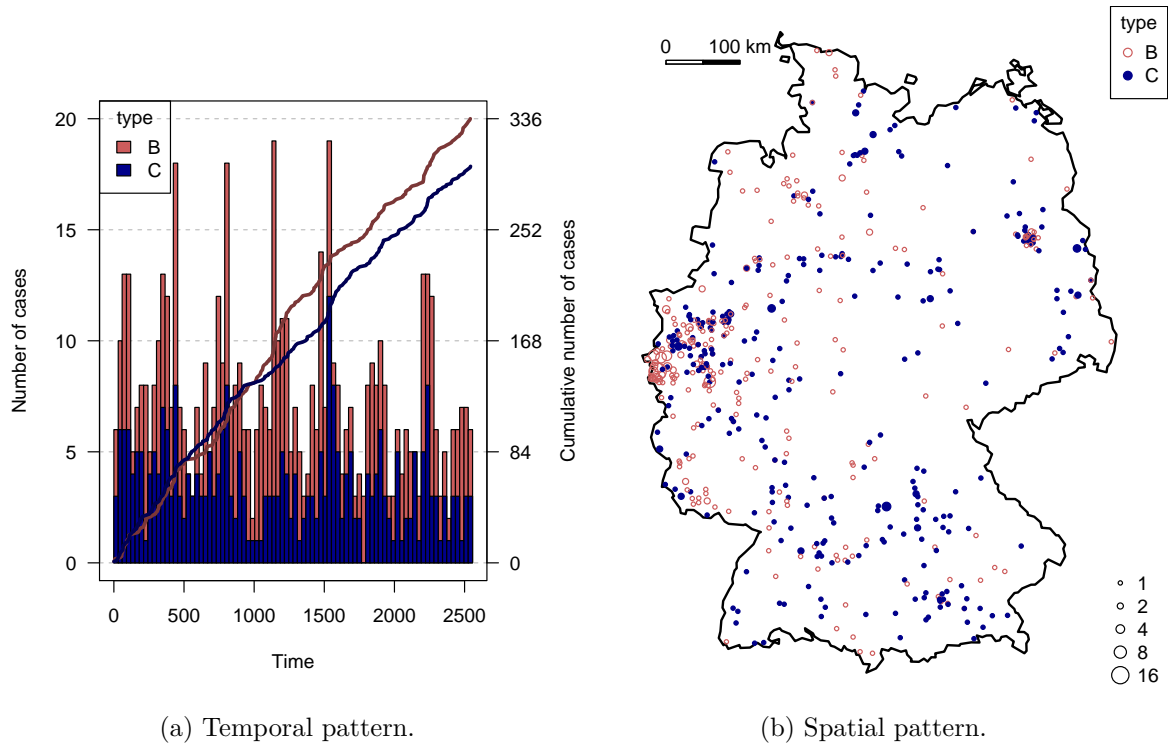
(a) Temporal pattern.

(b) Spatial pattern.

Figure 2: Occurrence of the two finetypes viewed in the temporal and spatial dimensions.

The above static plots do not capture the space-time dynamics of epidemic spread. An animation may provide additional insight and can be produced by the corresponding `animate`-method. For instance, to look at the first year of the B-type in a weekly sequence of snapshots in a web browser (using facilities of the **animation** package of Xie 2013):

```
R> animation::saveHTML(
+    animate(subset(imdepi, type == "B"), interval = c(0, 365), time.spacing = 7),
+    nmax = Inf, interval = 0.2, loop = FALSE,
+    title = "Animation of the first year of type B events")
```

Selecting events from `epidataCS` as for the animation above is enabled by the `[`- and `subset`-methods, which return a new `epidataCS` object containing only the selected `events`.

A limited data sampling resolution may lead to tied event times or locations, which are in conflict with a continuous spatio-temporal point process model. For instance, a temporal residual analysis would suggest model deficiencies (Meyer *et al.* 2012, Figure 4), and a power-law kernel for spatial interaction may diverge if there are events with zero distance to potential source events (Meyer and Held 2014a). The function `untie` breaks ties by random shifts. This has already been applied to the event *times* in the provided `imdepi` data by subtracting a U(0,1)-distributed random number from the original dates. The event *coordinates* in the IMD data are subject to interval censoring at the level of Germany's postcode regions. A possible replacement for the given centroids would thus be a random location within the corresponding postcode area. Lacking a suitable shapefile, Meyer and Held (2014a) shifted all locations by a random vector with length up to half the observed minimum spatial separation:

```
R> eventDists <- dist(coordinates(imdepi$events))
R> (minsep <- min(eventDists[eventDists > 0]))
```

```
[1] 1.17
```

```
R> set.seed(321)
R> imdepi_untied <- untie(imdepi, amount = list(s = minsep / 2))
```

Note that random tie-breaking requires sensitivity analyses as discussed by Meyer and Held (2014a), but skipped here for the sake of brevity.

The update-method is useful to change the values of the maximum interaction ranges eps.t and eps.s, since it takes care of the necessary updates of the hidden auxiliary variables in an epidataCS object. For an unbounded interaction radius:

```
R> imdepi_untied_infeps <- update(imdepi_untied, eps.s = Inf)
```

Last but not least, epidataCS can be converted to the other classes epidata (Section 4) and sts (Section 5) by aggregation. The method as.epidata.epidataCS aggregates events by region (tile), and the function epidataCS2sts yields counts by region and time interval. The data could then, e.g., be analyzed by the multivariate time-series model presented in Section 5. We can also use visualization tools of the sts class, e.g., to produce Figure 3:

```
R> imdsts <- epidataCS2sts(imdepi, freq = 12, start = c(2002, 1), tiles = districtsD)
R> plot(imdsts, type = observed ~ time)
R> plot(imdsts, type = observed ~ unit, population = districtsD$POPULATION / 100000)
```
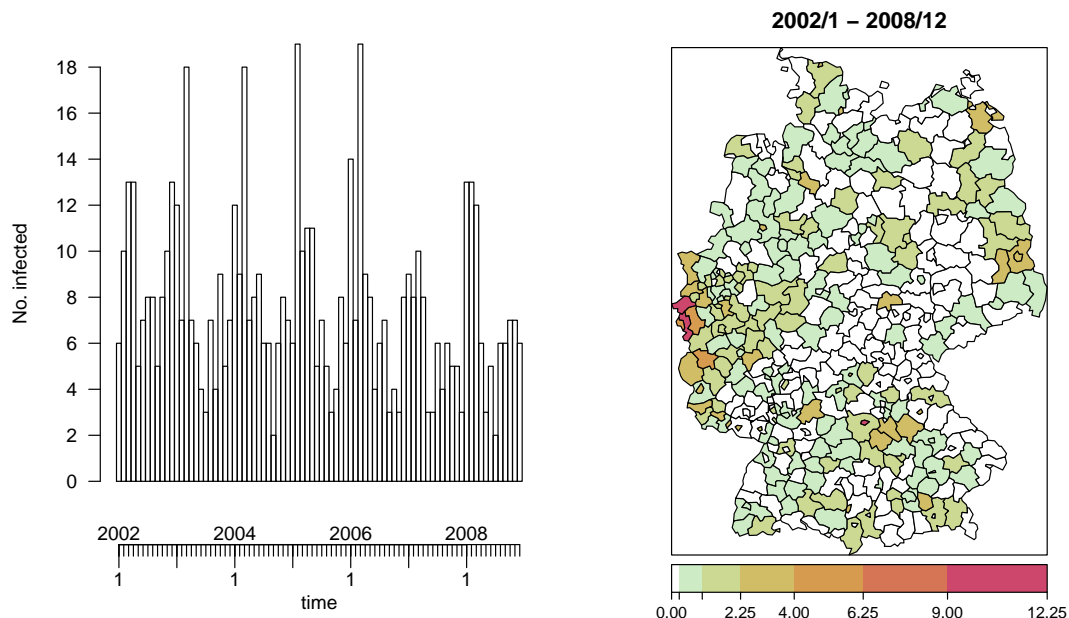

(a) Time series of monthly counts.　　　(b) Disease incidence (per 100 000 inhabitants).

Figure 3: IMD cases (joint types) aggregated as an sts object by month and district.

3.3. Modeling and inference

Having prepared the data as an object of class `epidataCS`, the function `twinstim` can be used to perform likelihood inference for conditional intensity models of the form (2). The main arguments for `twinstim` are the formulae of the `endemic` and `epidemic` linear predictors ($\nu_{[s][t]} = \exp(\text{endemic})$ and $\eta_j = \exp(\text{epidemic})$), and the spatial and temporal interaction functions `siaf` (f) and `tiaf` (g), respectively. Both formulae are parsed internally using the standard `model.frame` toolbox from package **stats** and thus can handle factor variables and interaction terms. While the `endemic` linear predictor incorporates time-dependent and/or areal-level covariates from `stgrid`, the `epidemic` formula may use both `stgrid` variables and event marks to be associated with the force of infection. For the interaction functions, several alternatives are predefined as listed in Table 3. They are applicable out-of-the-box and illustrated as part of the following modeling exercise for the IMD data. Own interaction functions can also be used provided their implementation obeys a certain structure, see `help("siaf")` and `help("tiaf")`, respectively.

Spatial (`siaf.*`)	Temporal (`tiaf.*`)
constant	constant
gaussian	exponential
powerlaw	step
powerlawL	
step	
student	

Table 3: Predefined spatial and temporal interaction functions.

Basic example

To illustrate statistical inference with `twinstim`, we will estimate several models for the simplified and "untied" IMD data presented in Section 3.2. In the endemic component, we include the district-specific population density as a multiplicative offset, a (centered) time trend, and a sinusoidal wave of frequency $2\pi/365$ to capture seasonality, where the `start` variable from `stgrid` measures time:

```
R> (endemic <- addSeason2formula(~offset(log(popdensity)) + I(start / 365 - 3.5),
+    period = 365, timevar = "start"))

~offset(log(popdensity)) + I(start/365 - 3.5) + sin(2 * pi *
    start/365) + cos(2 * pi * start/365)
```

See Held and Paul (2012, Section 2.2) for how such sine/cosine terms reflect seasonality. Because of the aforementioned integrations in the log-likelihood (5), it is advisable to first fit an endemic-only model to obtain reasonable start values for more complex epidemic models:

```
R> imdfit_endemic <- twinstim(endemic = endemic, epidemic = ~0,
+    data = imdepi_untied, subset = !is.na(agegrp))
```

We exclude the single case with unknown age group from this analysis since we will later estimate an effect of the age group on the force of infection.

Display	Extract	Modify	Other
print	nobs	update	simulate
summary	vcov	add1	*epitest*
xtable	coeflist	drop1	
plot	logLik	*stepComponent*	
intensityplot	extractAIC		
iafplot	profile		
checkResidualProcess	residuals		
	terms		
	R0		

Table 4: Generic and *non-generic* functions applicable to `twinstim` objects. Note that there is no need for specific `coef`, `confint`, `AIC` or `BIC` methods, since the respective default methods from package **stats** apply outright.

Many of the standard functions to access model fits in R are also implemented for `twinstim` fits (see Table 4). For example, we can produce the usual model summary:

```
R> summary(imdfit_endemic)


Call:
twinstim(endemic = endemic, epidemic = ~0, data = imdepi_untied,
    subset = !is.na(agegrp))

Coefficients of the endemic component:
                        Estimate Std. Error z value Pr(>|z|)
h.(Intercept)           -20.3683     0.0419 -486.24  < 2e-16 ***
h.I(start/365 - 3.5)     -0.0444     0.0200   -2.22    0.027 *
h.sin(2 * pi * start/365) 0.2733     0.0576    4.75  2.0e-06 ***
h.cos(2 * pi * start/365) 0.3509     0.0581    6.04  1.5e-09 ***
---
Signif. codes:  0 '***' 0.001 '**' 0.01 '*' 0.05 '.' 0.1 ' ' 1

No epidemic component.

AIC:  19166
Log-likelihood: -9579
```

Because of the aforementioned equivalence of the endemic component with a Poisson regression model, the coefficients can be interpreted as log rate ratios in the usual way. For instance, the endemic rate is estimated to decrease by `1 - exp(coef(imdfit_endemic)[2])` = 4.3% per year. Coefficient correlations can be retrieved by the argument `correlation = TRUE` in the `summary` call just like for `summary.glm`, but may also be extracted via the standard `cov2cor(vcov(imdfit_endemic))`.

We now update the endemic model to take additional spatio-temporal dependence between events into account. Infectivity shall depend on the meningococcal finetype and the age group of the patient, and is assumed to be constant over time (default), $g(t) = \mathbb{1}_{(0,30]}(t)$, with a Gaussian distance-decay $f(x) = \exp\{-x^2/(2\sigma^2)\}$. This model was originally selected by Meyer *et al.* (2012) and can be fitted as follows:

```
R> imdfit_Gaussian <- update(imdfit_endemic, epidemic = ~type + agegrp,
+    siaf = siaf.gaussian(), start = c("e.(Intercept)" = -12.5, "e.siaf.1" = 2.75),
+    control.siaf = list(F = list(adapt = 0.25), Deriv = list(nGQ = 13)),
+    cores = 2 * (.Platform$OS.type == "unix"), model = TRUE)
```

To reduce the runtime of this example, we specified convenient `start` values for some parameters (others start at 0) and set `control.siaf` with a rather low number of nodes for the cubature of $f(\|s\|)$ in the log-likelihood (via the midpoint rule) and $\frac{\partial f(\|s\|)}{\partial \log \sigma}$ in the score function (via product Gauss cubature). On Unix-alikes, these numerical integrations can be performed in parallel using the "multicore" functions `mclapply` *et al.* from the base package **parallel**, here with `cores = 2` processes. For later generation of an `intensityplot`, the `model` environment is retained.

	RR	95% CI	p-value
h.I(start/365 - 3.5)	0.955	0.91–1.00	0.039
h.sin(2 * pi * start/365)	1.243	1.09–1.41	0.0008
h.cos(2 * pi * start/365)	1.375	1.21–1.56	<0.0001
e.typeC	0.402	0.24–0.68	0.0007
e.agegrp[3,19)	2.000	1.06–3.78	0.033
e.agegrp[19,Inf)	0.776	0.32–1.91	0.58

Table 5: Estimated rate ratios (RR) and associated Wald confidence intervals (CI) for endemic (`h.`) and epidemic (`e.`) terms. This table was generated by `xtable(imdfit_Gaussian)`.

Table 5 shows the output of `twinstim`'s `xtable` method (Dahl 2015), which provides rate ratios for the endemic and epidemic effects. The alternative `toLatex` method simply translates the `summary` table of coefficients to LaTeX without `exp`-transformation. On the subject-matter level, we can conclude from Table 5 that the meningococcal finetype of serogroup C is less than half as infectious as the B-type, and that patients in the age group 3 to 18 years are estimated to cause twice as many secondary infections as infants aged 0 to 2 years.

Model-based effective reproduction numbers

The event-specific reproduction numbers (3) can be extracted from fitted `twinstim` objects via the `R0` method. For the above IMD model, we obtain the following mean numbers of secondary infections by finetype:

```
R> R0_events <- R0(imdfit_Gaussian)
R> tapply(R0_events, marks(imdepi_untied)[names(R0_events), "type"], mean)


     B      C
0.2161 0.0958
```

Confidence intervals can be obtained via Monte Carlo simulation, where Equation 3 is repeatedly evaluated with parameters sampled from the asymptotic multivariate normal distribution of the maximum likelihood estimate. For this purpose, the `R0`-method takes an argument `newcoef`, which is exemplified in `help("R0")`.

Interaction functions

Figure 4 shows several estimated spatial interaction functions, which can be plotted by, e.g., `plot(imdfit_Gaussian, which = "siaf")`. Meyer and Held (2014a) found that a power-law decay of spatial interaction is more appropriate than a Gaussian kernel to describe the spread of human infectious diseases. The power-law kernel concentrates on short-range interaction, but also exhibits a heavier tail reflecting occasional transmission over large distances. To use the power-law kernel $f(x) = (x + \sigma)^{-d}$, we switch to the prepared `epidataCS` object with `eps.s = Inf` and update the previous Gaussian model as follows:

```
R> imdfit_powerlaw <- update(imdfit_Gaussian, data = imdepi_untied_infeps,
+    siaf = siaf.powerlaw(), control.siaf = NULL,
+    start = c("e.(Intercept)" = -6.2, "e.siaf.1" = 1.5, "e.siaf.2" = 0.9))
```

Table 3 also lists the step function kernel as an alternative, which is particularly useful for two reasons. First, it is a more flexible approach since it estimates interaction between the given knots without assuming an overall functional form. Second, the spatial integrals in the log-likelihood can be computed analytically for the step function kernel, which therefore offers a quick estimate of spatial interaction. We update the Gaussian model to use four steps at log-equidistant knots up to an interaction range of 100 km:

```
R> imdfit_step4 <- update(imdfit_Gaussian, data = imdepi_untied_infeps,
+    siaf = siaf.step(exp(1:4 * log(100) / 5), maxRange = 100), control.siaf = NULL,
+    start = c("e.(Intercept)" = -10, setNames(-2:-5, paste0("e.siaf.", 1:4))))
```

Figure 4 suggests that the estimated step function is in line with the power law.

For the temporal interaction function $g(t)$, model updates and plots are similarly possible, e.g., `update(imdfit_Gaussian, tiaf = tiaf.exponential())`. However, the events in the IMD data are too rare to infer the time-course of infectivity with confidence.
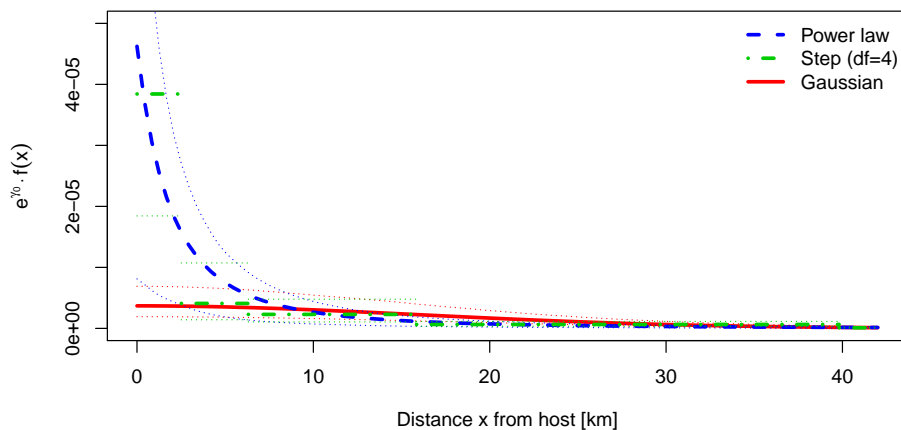

Figure 4: Various estimates of spatial interaction (scaled by the epidemic intercept γ_0). The standard deviation of the Gaussian kernel is estimated to be $\hat{\sigma} = 16.00$ (95% CI: 13.65–18.75), and the estimated power-law parameters are $\hat{\sigma} = 4.64$ (95% CI: 1.82–11.84) and $\hat{d} = 2.49$ (95% CI: 1.81–3.42).

Model selection

```
R> AIC(imdfit_endemic, imdfit_Gaussian, imdfit_powerlaw, imdfit_step4)

                df   AIC
imdfit_endemic    4 19166
imdfit_Gaussian   9 18967
imdfit_powerlaw  10 18940
imdfit_step4     12 18933
```

Akaike's Information Criterion (AIC) suggests superiority of the power-law vs. the Gaussian model and the endemic-only model. The more flexible step function yields the best AIC value but its shape strongly depends on the chosen knots and is not guaranteed to be monotonically decreasing. The function `stepComponent` – a wrapper around the `step` function from **stats** – can be used to perform AIC-based stepwise selection within a given model component.

Model diagnostics

Two other plots are implemented for `twinstim` objects. Figure 5 shows an `intensityplot` of the fitted "ground" intensity $\sum_{k=1}^{2} \int_{W} \hat{\lambda}(\boldsymbol{s}, t, k) \, \mathrm{d}\boldsymbol{s}$ aggregated over both event types:

```
R> intensityplot(imdfit_powerlaw, which = "total", aggregate = "time", types = 1:2)
```
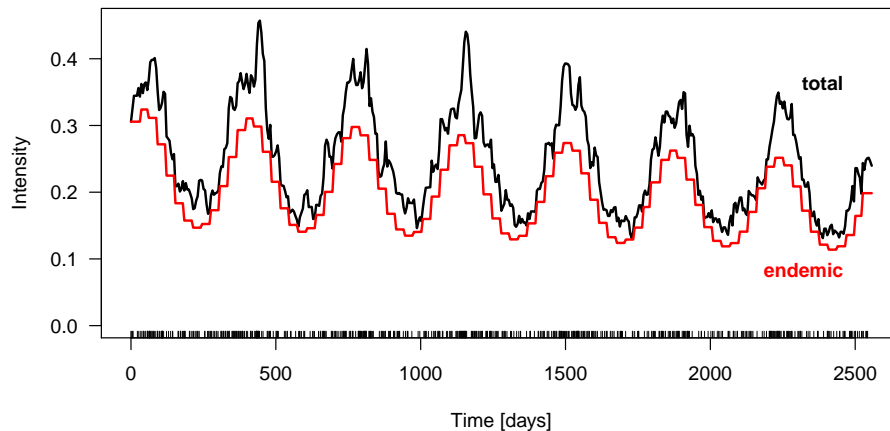

Figure 5: Fitted "ground" intensity process aggregated over space and both types.

The estimated endemic intensity component has also been added to the plot. It exhibits strong seasonality and a slow negative trend. The proportion of the endemic intensity is rather constant along time since no major outbreaks occurred. This proportion can be visualized separately by specifying `which = "endemic proportion"` in the above call.

Spatial `intensityplots` can be produced via `aggregate = "space"` and require a geographic representation of `stgrid`. Figure 6 shows the accummulated epidemic proportion by event type. It is naturally high in regions with a large number of cases and even more so if the population density is low. The function `epitest` offers a model-based global test for epidemicity, while `knox` and `stKtest` implement related classical approaches (Meyer *et al.* 2015).
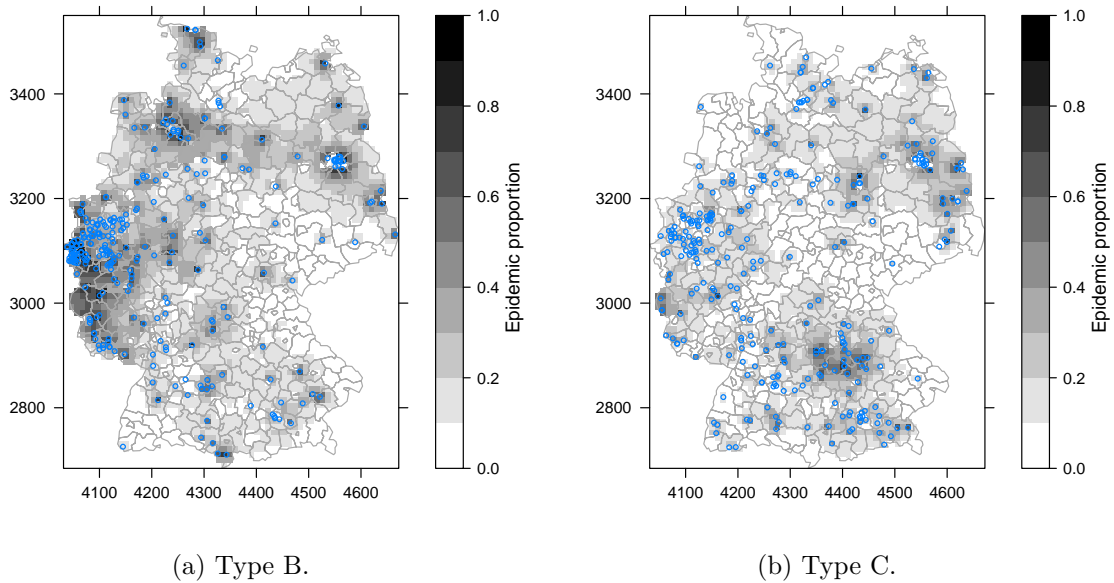
(a) Type B. (b) Type C.

Figure 6: Epidemic proportion of the fitted intensity process accumulated over time by type.

Another diagnostic tool is the function `checkResidualProcess`, which transforms the temporal "residual process" in such a way that it exhibits a uniform distribution and lacks serial correlation if the fitted model describes the true CIF well (see Ogata 1988, Section 3.3). These properties can be checked graphically as in Figure 7 produced by:

```
R> checkResidualProcess(imdfit_powerlaw)
```
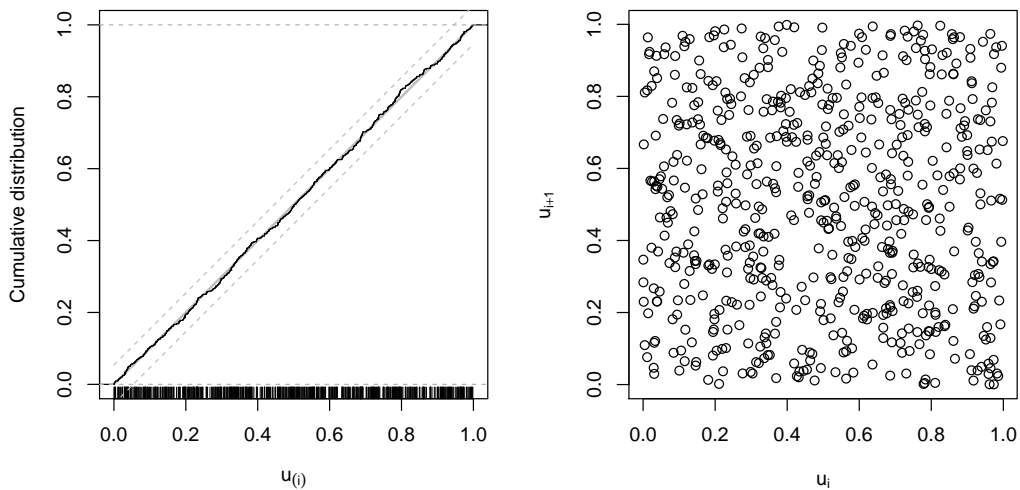

Figure 7: The left plot shows the `ecdf` of the transformed residuals with a 95% confidence band obtained by inverting the corresponding Kolmogorov-Smirnov test (no evidence for deviation from uniformity). The right-hand plot suggests absence of serial correlation.

3.4. Simulation

To identify regions with unexpected IMD dynamics, Meyer *et al.* (2012) compared the observed numbers of cases by district to the respective 2.5% and 97.5% quantiles of 100 simulations from the selected model. Furthermore, simulations allow us to investigate the stochastic volatility of the endemic-epidemic process, to obtain probabilistic forecasts, and to perform parametric bootstrap of the spatio-temporal point pattern.

The simulation algorithm we apply is described in Meyer *et al.* (2012, Section 4). It requires a geographic representation of the `stgrid`, as well as functionality for sampling locations from the spatial kernel $f_2(s) := f(\|s\|)$. This is implemented for all predefined spatial interaction functions listed in Table 3. Event marks are by default sampled from their respective empirical distribution in the original data. The following code runs 30 simulations over the last two years based on the estimated power-law model:

```
R> imdsims <- simulate(imdfit_powerlaw, nsim = 30, seed = 1, t0 = 1826, T = 2555,
+    data = imdepi_untied_infeps, tiles = districtsD)
```

Figure 8 shows the cumulative number of cases from the simulations appended to the first five years of data. Extracting a single simulation (e.g., `imdsims[[1]]`) yields an object of the class `simEpidataCS`, which extends `epidataCS`. It carries additional components from the generating model to enable an `R0`-method and `intensityplot`s for simulated data. A special feature of such simulations is that the source of each event is actually known:

```
R> table(imdsims[[1]]$events$source > 0, exclude = NULL)


FALSE   TRUE   <NA>
  112     25      8
```

The stored `source` value is 0 for endemic events, `NA` for events of the prehistory but still infective at `t0`, and otherwise corresponds to the row index of the infective source. Averaged over all 30 simulations, the proportion of events triggered by previous events is 0.218.
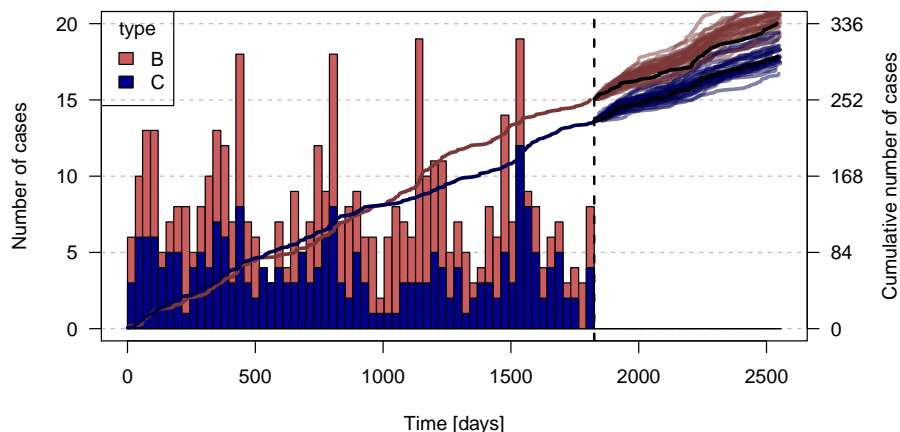

Figure 8: Simulation-based forecast of the cumulative number of cases by finetype in the last two years. The black lines correspond to the observed numbers.

4. SIR event history of a fixed population

The endemic-epidemic multivariate point process model "`twinSIR`" is designed for individual-level surveillance data of a fixed population of which the complete SIR event history is assumed to be known. As an illustrative example, we use a particularly well-documented measles outbreak among children of the isolated German village Hagelloch in the year 1861, which has previously been analyzed by, e.g., Neal and Roberts (2004). Other potential applications include farm-level data as well as epidemics across networks. We start by describing the general model class in Section 4.1. Section 4.2 introduces the example data and the associated class `epidata`, and Section 4.3 presents the core functionality of fitting and analyzing such data using `twinSIR`. Due to the many similarities with the `twinstim` framework covered in Section 3, we condense the `twinSIR` treatment accordingly.

4.1. Model class: `twinSIR`

The previously described point process model `twinstim` (Section 3) is indexed in a continuous spatial domain, i.e., the set of possible event locations consists of the whole observation region and is thus infinite. However, if infections can only occur at a known discrete set of sites, such as for livestock diseases among farms, the conditional intensity function formally becomes $\lambda_i(t)$. It characterizes the instantaneous rate of infection of individual i at time t, given the sets $S(t)$ and $I(t)$ of susceptible and infectious individuals, respectively (just before time t). In a similar regression view as in Section 3, Höhle (2009) proposed the endemic-epidemic multivariate temporal point process "`twinSIR`":

$$\lambda_i(t) = \lambda_0(t)\,\nu_i(t) + \sum_{j \in I(t)} \left\{ f(d_{ij}) + \boldsymbol{w}_{ij}^\top \boldsymbol{\alpha}^{(w)} \right\}, \tag{6}$$

if $i \in S(t)$, i.e., if individual i is currently susceptible, and $\lambda_i(t) = 0$ otherwise. The rate decomposes into two components. The endemic component consists of a Cox proportional hazards formulation containing a semi-parametric baseline hazard $\lambda_0(t)$ and a log-linear predictor $\nu_i(t) = \exp\left(\boldsymbol{z}_i(t)^\top \boldsymbol{\beta} \right)$ of covariates modeling infection from external sources. Furthermore, an additive epidemic component captures transmission from the set $I(t)$ of currently infectious individuals. The force of infection of individual i depends on the distance d_{ij} to each infective source $j \in I(t)$ through a distance kernel

$$f(u) = \sum_{m=1}^{M} \alpha_m^{(f)} B_m(u) \ge 0, \tag{7}$$

which is represented by a linear combination of non-negative basis functions B_m with the $\alpha_m^{(f)}$'s being the respective coefficients. For instance, f could be modelled by a B-spline (Fahrmeir, Kneib, Lang, and Marx 2013, Section 8.1), and d_{ij} could refer to the Euclidean distance $\|\boldsymbol{s}_i - \boldsymbol{s}_j\|$ between the individuals' locations $\boldsymbol{s}_i$ and $\boldsymbol{s}_j$, or to the geodesic distance between the nodes i and j in a network. The distance-based force of infection is modified additively by a linear predictor of covariates $\boldsymbol{w}_{ij}$ describing the interaction of individuals i and j further. Hence, the whole epidemic component of Equation 6 can be written as a single linear predictor $\boldsymbol{x}_i(t)^\top \boldsymbol{\alpha}$ by interchanging the summation order to

$$\sum_{m=1}^{M} \alpha_m^{(f)} \sum_{j \in I(t)} B_m(d_{ij}) + \sum_{k=1}^{K} \alpha_k^{(w)} \sum_{j \in I(t)} w_{ijk} = \boldsymbol{x}_i(t)^\top \boldsymbol{\alpha}, \tag{8}$$

such that $\boldsymbol{x}_i(t)$ comprises all epidemic terms summed over $j \in I(t)$. Note that the use of additive covariates $\boldsymbol{w}_{ij}$ on top of the distance kernel in (6) is different from `twinstim`'s multiplicative approach in (2). One advantage of the additive approach is that the subsequent linear decomposition of the distance kernel allows one to gather all parts of the epidemic component in a single linear predictor. Hence, the above model represents a CIF extension of what in the context of survival analysis is known as an additive-multiplicative hazard model (Martinussen and Scheike 2002). As a consequence, the `twinSIR` model could in principle be fitted with the **timereg** package (Scheike and Martinussen 2006), which yields estimates for the cumulative hazards. However, Höhle (2009) chooses a more direct inferential approach: To ensure that the CIF $\lambda_i(t)$ is non-negative, all covariates are encoded such that the components of $\boldsymbol{w}_{ij}$ are non-negative. Additionally, the parameter vector $\boldsymbol{\alpha}$ is constrained to be non-negative. Subsequent parameter inference is then based on the resulting constrained penalized likelihood which gives directly interpretable estimates of $\boldsymbol{\alpha}$.

4.2. Data structure: `epidata`

New SIR-type event data typically arrive in the form of a simple data frame with one row per individual and the time points of the sequential events of the individual as columns. For the 1861 Hagelloch measles epidemic, such a data set of the 188 affected children is contained in the **surveillance** package:

```
R> data("hagelloch")
R> head(hagelloch.df, n = 5)
```

```
  PN    NAME FN HN AGE    SEX        PRO        ERU        CL DEAD IFTO SI
1  1 Mueller 41 61   7 female 1861-11-21 1861-11-25 1st class <NA>   45 10
2  2 Mueller 41 61   6 female 1861-11-23 1861-11-27 1st class <NA>   45 12
3  3 Mueller 41 61   4 female 1861-11-28 1861-12-02 preschool <NA>  172  9
4  4 Seibold 61 62  13   male 1861-11-27 1861-11-28 2nd class <NA>  180 10
5  5  Motzer 42 63   8 female 1861-11-22 1861-11-27 1st class <NA>   45 11
                C PR CA NI GE TD   TM x.loc y.loc tPRO tERU tDEAD   tR   tI
1 no complicatons  4  4  3  1 NA   NA   142   100 22.7 26.2    NA 29.2 21.7
2 no complicatons  4  4  3  1  3 40.3   142   100 24.2 28.8    NA 31.8 23.2
3 no complicatons  4  4  3  2  1 40.5   142   100 29.6 33.7    NA 36.7 28.6
4 no complicatons  1  1  1  1  3 40.7   165   102 28.1 29.0    NA 32.0 27.1
5 no complicatons  5  3  2  1 NA   NA   145   120 23.1 28.4    NA 31.4 22.1
```

The `help("hagelloch")` contains a description of all columns. Here we concentrate on the event columns `PRO` (appearance of prodromes), `ERU` (eruption), and `DEAD` (day of death if during the outbreak). We take the day on which the index case developed first symptoms, 30 October 1861 (`min(hagelloch.df$PRO)`), as the start of the epidemic, i.e., we condition on this case being initially infectious. As for `twinstim`, the property of point processes that concurrent events have zero probability requires special treatment. Ties are due to the interval censoring of the data to a daily basis – we broke these ties by adding random jitter to the event times within the given days. The resulting columns `tPRO`, `tERU`, and `tDEAD` are relative to the defined start time. Following Neal and Roberts (2004), we assume that each child becomes infectious (S → I event at time `tI`) one day before the appearance of prodromes, and is removed from the epidemic (I → R event at time `tR`) three days after the appearance of rash or at the time of death, whichever comes first.

For further processing of the data, we convert `hagelloch.df` to the standardized `epidata` structure for `twinSIR`. This is done by the converter function `as.epidata`, which also checks consistency and optionally pre-calculates the epidemic terms $x_i(t)$ of Equation 8 to be incorporated in a `twinSIR` model. The following call generates the `epidata` object `hagelloch`:

```
R> hagelloch <- as.epidata(hagelloch.df,
+    t0 = 0, tI.col = "tI", tR.col = "tR",
+    id.col = "PN", coords.cols = c("x.loc", "y.loc"),
+    f = list(household    = function(u) u == 0,
+             nothousehold = function(u) u > 0),
+    w = list(c1 = function (CL.i, CL.j) CL.i == "1st class" & CL.j == CL.i,
+             c2 = function (CL.i, CL.j) CL.i == "2nd class" & CL.j == CL.i),
+    keep.cols = c("SEX", "AGE", "CL"))
```

The coordinates (`x.loc`, `y.loc`) correspond to the location of the household the child lives in and are measured in meters. Note that `twinSIR` allows for tied locations of individuals, but assumes the relevant spatial location to be fixed during the entire observation period. By default, the Euclidean distance between the given coordinates will be used. Alternatively, `as.epidata` also accepts a pre-computed distance matrix via its argument `D` without requiring spatial coordinates. The argument `f` lists distance-dependent basis functions B_m for which the epidemic terms $\sum_{j \in I(t)} B_m(d_{ij})$ shall be generated. Here, `household` ($x_{i,H}(t)$) and `nothousehold` ($x_{i,\bar{H}}(t)$) count for each child the number of currently infective children in its household and outside its household, respectively. Similar to Neal and Roberts (2004), we also calculate the covariate-based epidemic terms `c1` ($x_{i,c1}(t)$) and `c2` ($x_{i,c2}(t)$) counting the number of currently infective classmates. Note from the corresponding definitions of w_{ij1} and w_{ij2} in `w` that `c1` is always zero for children of the second class and `c2` is always zero for children of the first class. For pre-school children, both variables equal zero over the whole period. By the last argument `keep.cols`, we choose to only keep the covariates `SEX`, `AGE`, and school `CLass` from `hagelloch.df`.

The first few rows of the generated `epidata` object are shown below:

```
R> head(hagelloch, n = 5)
```

```
  BLOCK id start stop atRiskY event Revent x.loc y.loc    SEX AGE        CL
1     1  1     0 1.14       1     0      0   142   100 female   7 1st class
2     1  2     0 1.14       1     0      0   142   100 female   6 1st class
3     1  3     0 1.14       1     0      0   142   100 female   4 preschool
4     1  4     0 1.14       1     0      0   165   102   male  13 2nd class
5     1  5     0 1.14       1     0      0   145   120 female   8 1st class
  household nothousehold c1 c2
1         0            1  0  0
2         0            1  0  0
3         0            1  0  0
4         0            1  0  1
5         0            1  0  0
```

The `epidata` structure inherits from counting processes as implemented by the `Surv` class of package **survival** (Therneau 2015) and also used in, e.g., the **timereg** package (Scheike and Zhang 2011). Specifically, the observation period is splitted up into consecutive time intervals

(`start`; `stop`] of constant conditional intensities. As the CIF $\lambda_i(t)$ of Equation (6) only changes at time points, where the set of infectious individuals $I(t)$ or some endemic covariate in $\nu_i(t)$ change, those occurrences define the break points of the time intervals. Altogether, the `hagelloch` event history consists of 375 time `BLOCK`s of 188 rows, where each row describes the state of individual `id` during the corresponding time interval. The susceptibility status and the I- and R-events are captured by the columns `atRiskY`, `event` and `Revent`, respectively. The `atRiskY` column indicates if the individual is at risk of becoming infected in the current interval. The event columns indicate, which individual was infected or removed at the `stop` time. Note that at most one entry in the `event` and `Revent` columns is 1, all others are 0.

Apart from being the input format for `twinSIR` models, the `epidata` class has several associated methods (Table 6), which are similar in spirit to the methods described for `epidataCS`.

Display	Subset	Modify
print	[	update
summary		
plot		
animate		
stateplot		

Table 6: Generic and *non-generic* functions applicable to `epidata` objects.

For example, Figure 9 illustrates the course of the Hagelloch measles epidemic by counting processes for the number of susceptible, infectious and removed children, respectively. Figure 10 shows the locations of the households. An `animate`d map can also be produced to view the households' states over time and a `stateplot` shows the changes for a selected unit.

```
R> plot(hagelloch, xlab = "Time [days]")
```
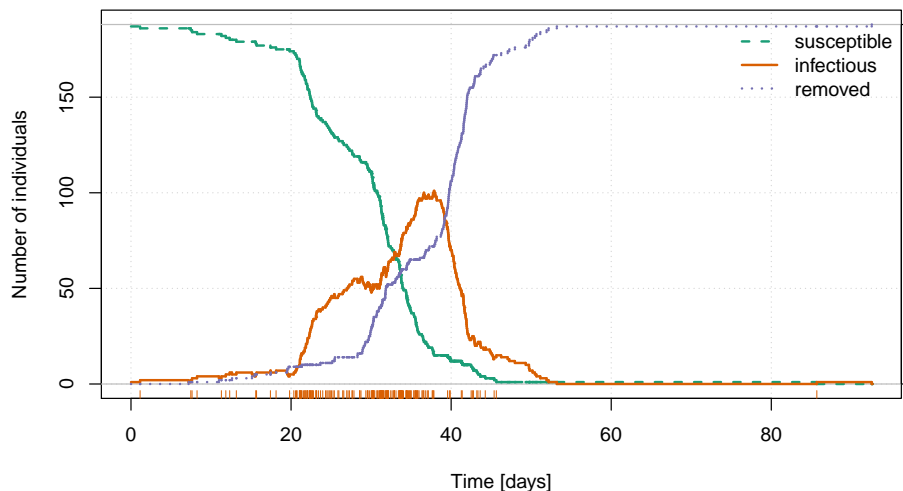

Figure 9: Evolution of the 1861 Hagelloch measles epidemic in terms of the numbers of susceptible, infectious, and recovered children. The bottom `rug` marks the infection times `tI`.

```
R> hagelloch_coords <- summary(hagelloch)$coordinates
R> plot(hagelloch_coords, xlab = "x [m]", ylab = "y [m]",
+    pch = 15, asp = 1, cex = sqrt(multiplicity(hagelloch_coords)))
R> legend(x = "topleft", pch = 15, legend = c(1, 4, 8), pt.cex = sqrt(c(1, 4, 8)),
+    title = "Household size")
```
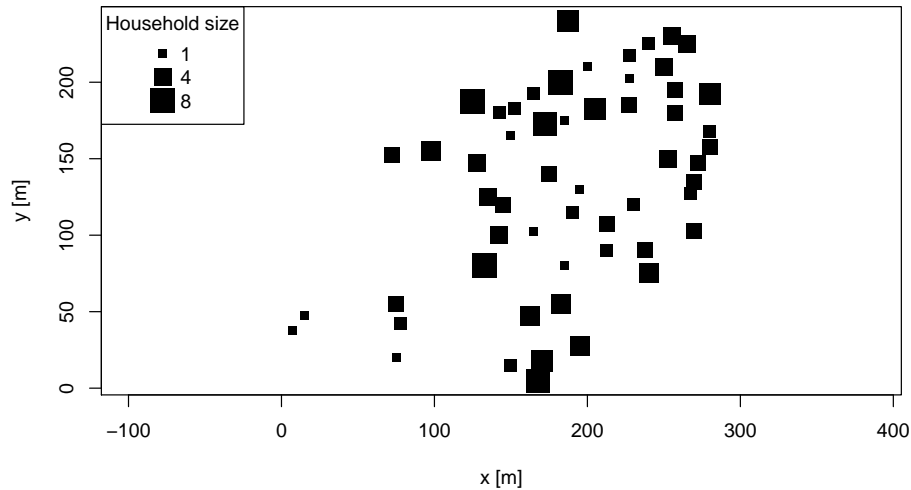

Figure 10: Spatial locations of the Hagelloch households. The size of each dot is proportional to the number of children in the household.

4.3. Modeling and inference

Basic example

To illustrate the flexibility of `twinSIR` we will analyze the Hagelloch data using class room and household indicators similar to Neal and Roberts (2004). We include an additional endemic background rate $\exp(\beta_0)$, which allows for multiple outbreaks triggered by external sources. Consequently, we do not need to ignore the child that got infected about one month after the end of the main epidemic (see the last event mark in Figure 9), as, e.g., done in a thorough network-based analysis of the Hagelloch data by Groendyke, Welch, and Hunter (2012). Altogether, the CIF for a child i is modeled as

$$\lambda_i(t) = Y_i(t) \cdot \left[\exp(\beta_0) + \alpha_H x_{i,H}(t) + \alpha_{c1} x_{i,c1}(t) + \alpha_{c2} x_{i,c2}(t) + \alpha_{\bar{H}} x_{i,\bar{H}}(t) \right] , \qquad (9)$$

where $Y_i(t) = \mathbb{1}(i \in S(t))$ is the at-risk indicator. By counting the number of infectious classmates separately for both school classes as described in the previous section, we allow for class-specific effects α_{c1} and α_{c2} on the force of infection. The model is estimated by maximum likelihood (Höhle 2009) using the following call:

```
R> hagellochFit <- twinSIR(~household + c1 + c2 + nothousehold, data = hagelloch)
R> summary(hagellochFit)
```

```
Call:
twinSIR(formula = ~household + c1 + c2 + nothousehold, data = hagelloch)

Coefficients:
                 Estimate Std. Error z value Pr(>|z|)
household        0.026868   0.006113    4.39  1.1e-05 ***
c1               0.023892   0.005026    4.75  2.0e-06 ***
c2               0.002932   0.000755    3.88   0.0001 ***
nothousehold     0.000831   0.000142    5.87  4.3e-09 ***
cox(logbaseline) -7.362644   0.887989   -8.29  < 2e-16 ***
---
Signif. codes:  0 '***' 0.001 '**' 0.01 '*' 0.05 '.' 0.1 ' ' 1

Total number of infections:  187

One-sided AIC: 1245        (simulated penalty weights)
Log-likelihood: -619
Number of log-likelihood evaluations: 119
```

The results show, e.g., a $0.0239 / 0.0029 = 8.15$ times higher transmission between individuals in the 1st class than in the 2nd class. Furthermore, an infectious housemate adds $0.0269 / 0.0008 = 32.3$ times as much infection pressure as infectious children outside the household. The endemic background rate of infection in a population with no current measles cases is estimated to be $\exp(\hat{\beta}_0) = \exp(-7.36) = 0.000635$. An associated Wald confidence interval (CI) based on the asymptotic normality of the maximum likelihood estimator (MLE) can be obtained by `exp`-transforming the `confint` for β_0:

```
R> exp(confint(hagellochFit, parm = "cox(logbaseline)"))


                    2.5 %  97.5 %
cox(logbaseline) 0.000111 0.00362
```

Note that Wald confidence intervals for the epidemic parameters $\boldsymbol{\alpha}$ are to be treated carefully, because their construction does not take the restricted parameter space into account. For more adequate statistical inference, the behavior of the log-likelihood near the MLE can be investigated using the `profile`-method for `twinSIR` objects. For instance, to evaluate the normalized profile log-likelihood of α_{c1} and α_{c2} on an equidistant grid of 25 points within the corresponding 95% Wald CIs, we do:

```
R> prof <- profile(hagellochFit,
+    list(c(match("c1", names(coef(hagellochFit))), NA, NA, 25),
+         c(match("c2", names(coef(hagellochFit))), NA, NA, 25)))
```

The profiling result contains 95% highest likelihood based CIs for the parameters, as well as the Wald CIs for comparison:

```
R> prof$ci.hl


   idx  hl.low  hl.up wald.low wald.up     mle
c1   2 0.01522 0.03497  0.01404 0.03374 0.02389
c2   3 0.00158 0.00454  0.00145 0.00441 0.00293
```

The entire functional form of the normalized profile log-likelihood on the requested grid as stored in `prof$lp` can be visualized by:
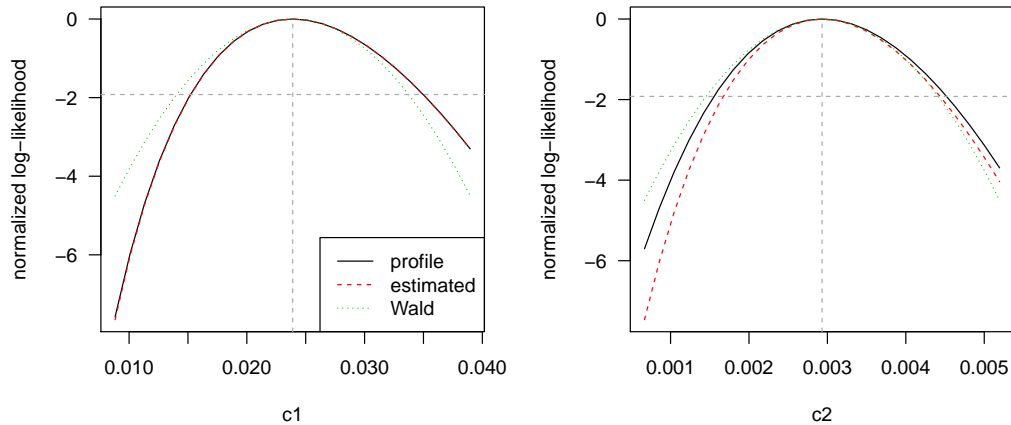
```
R> plot(prof)
```


Figure 11: Normalized log-likelihood for α_{c1} and α_{c2} when fitting the `twinSIR` model formulated in Equation (9) to the Hagelloch data.
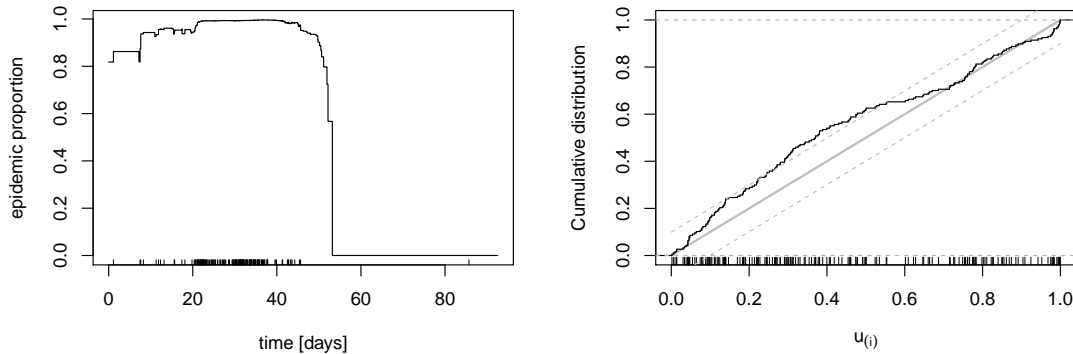
Model diagnostics

Display	Extract	Other
print	vcov	simulate
summary	logLik	
plot	AIC	
intensityplot	extractAIC	
checkResidualProcess	profile	
	residuals	

Table 7: Generic and *non-generic* functions for `twinSIR`. There are no specific `coef` or `confint` methods, since the respective default methods from package **stats** apply outright.

Table 7 lists all methods for the `twinSIR` class. For example, to investigate how the CIF decomposes into endemic and epidemic intensity over time, we produce Figure 12a by:

```
R> plot(hagellochFit, which = "epidemic proportion", xlab = "time [days]")
```

Note that the last infection was necessarily caused by the endemic component since there were no more infectious children in the observed population which could have triggered the new case. We can also inspect temporal Cox-Snell-like `residuals` of the fitted point process using the function `checkResidualProcess` as for the spatio-temporal point process models in Section 3.3. The resulting Figure 12b reveals some deficiencies of the model in describing the waiting times between events, which might be related to the assumption of fixed infection periods.

(a) Epidemic proportion.

(b) Transformed residuals.

Figure 12: Diagnostic plots for the `twinSIR` model formulated in Equation 9.

Finally, `twinSIR`'s `AIC`-method computes the one-sided AIC (Hughes and King 2003) as described in Höhle (2009), which can be used for model selection under positivity constraints on $\boldsymbol{\alpha}$. For instance, we may consider a more flexible model for local spread using a step function for the distance kernel $f(u)$ in Equation 7. An updated model with $B_1 = I_{(0;100)}(u)$, $B_2 = I_{[100;200)}(u)$, $B_3 = I_{[200;\infty)}(u)$ can be fitted as follows:

```
R> knots <- c(100, 200)
R> fstep <- list(
+    B1 = function(D) D > 0 & D < knots[1],
+    B2 = function(D) D >= knots[1] & D < knots[2],
+    B3 = function(D) D >= knots[2])
R> hagellochFit_fstep <- twinSIR(
+    ~household + c1 + c2 + B1 + B2 + B3,
+    data = update(hagelloch, f = fstep))

R> set.seed(1)
R> AIC(hagellochFit, hagellochFit_fstep)

                   df  AIC
hagellochFit        5 1245
hagellochFit_fstep  7 1246
```

Hence the simpler model with just a `nothousehold` component instead of the more flexible distance-based step function is preferred. A random seed was set since the parameter penalty in the one-sided AIC is determined by Monte Carlo simulation. The algorithm is described in Silvapulle and Sen (2005, p. 79, Simulation 3) and involves quadratic programming using package **quadprog** (Turlach 2013).

4.4. Simulation

Simulation from fitted `twinSIR` models is described in detail in Höhle (2009, Section 4). The implementation is made available by an appropriate `simulate`-method for class `twinSIR`. Because both the algorithm and the call are similar to the invocation on `twinstim` objects (Section 3.4), we skip the illustration here and refer to `help("simulate.twinSIR")`.

5. Areal time series of counts

In public health surveillance, routine reports of infections to public health authorities give rise to spatio-temporal data, which are usually made available in the form of aggregated counts by region and period. The Robert Koch Institute (RKI) in Germany, for example, maintains a database of cases of notifiable diseases, which can be queried via the *SurvStat@RKI*[4] online service. As an illustrative example, we use weekly counts of measles infections by district in the Weser-Ems region of Lower Saxony, Germany, 2001–2002. These spatio-temporal count data constitute the response Y_{it}, $i = 1, \ldots, 17$ (districts), $t = 1, \ldots, 104$ (weeks), for our illustration of the endemic-epidemic multivariate time-series model "`hhh4`". We start by describing the general model class in Section 5.1. Section 5.2 introduces the data and the associated `S4`-class `sts` ("surveillance time series"). In Section 5.3, a simple model for the measles data based on the original analysis of Held *et al.* (2005) is introduced, which is then sequentially improved by suitable model extensions. The final Section 5.4 illustrates simulation from fitted `hhh4` models.

5.1. Model class: `hhh4`

An endemic-epidemic multivariate time-series model for infectious disease counts Y_{it} from units $i = 1, \ldots, I$ during periods $t = 1, \ldots, T$ was proposed by Held *et al.* (2005) and was later extended in a series of papers (Paul *et al.* 2008; Paul and Held 2011; Held and Paul 2012; Meyer and Held 2014a). In its most general formulation, this so-called "`hhh4`" model assumes that, conditional on past observations, Y_{it} has a negative binomial distribution with mean

$$\mu_{it} = e_{it}\, \nu_{it} + \lambda_{it}\, Y_{i,t-1} + \phi_{it} \sum_{j \neq i} w_{ji}\, Y_{j,t-1} \tag{10}$$

and overdispersion parameter $\psi_i > 0$ such that the conditional variance of Y_{it} is $\mu_{it}(1 + \psi_i \mu_{it})$. Shared overdispersion parameters, e.g., $\psi_i \equiv \psi$, are supported as well as replacing the negative binomial by a Poisson distribution, which corresponds to the limit $\psi_i \equiv 0$.

Similar to the point process models of Sections 3 and 4, the mean (10) decomposes additively into endemic and epidemic components. The endemic mean is usually modelled proportional to an offset of expected counts e_{it}. In spatial applications of the multivariate `hhh4` model as in this paper, the "unit" i refers to a geographical region and we typically use (the fraction of) the population living in region i as the endemic offset. The observation-driven epidemic component splits up into autoregressive effects, i.e., reproduction of the disease within region i, and neighbourhood effects, i.e., transmission from other regions j. Overall, Equation 10 becomes a rich regression model by allowing for log-linear predictors in all three components:

$$\log(\nu_{it}) = \alpha_i^{(\nu)} + \boldsymbol{\beta}^{(\nu)\top} \boldsymbol{z}_{it}^{(\nu)} \,, \tag{11}$$

$$\log(\lambda_{it}) = \alpha_i^{(\lambda)} + \boldsymbol{\beta}^{(\lambda)\top} \boldsymbol{z}_{it}^{(\lambda)} \,, \tag{12}$$

$$\log(\phi_{it}) = \alpha_i^{(\phi)} + \boldsymbol{\beta}^{(\phi)\top} \boldsymbol{z}_{it}^{(\phi)} \,. \tag{13}$$

The intercepts of these predictors can be assumed identical across units, unit-specific, or random (and possibly correlated). The regression terms often involve sine-cosine effects of time to reflect seasonally varying incidence, but may, e.g., also capture heterogeneous vaccination

---

[4] https://survstat.rki.de

coverage (Herzog *et al.* 2011). Data on infections imported from outside the study region may enter the endemic component (Geilhufe *et al.* 2014), which generally accounts for cases not directly linked to other observed cases, e.g., due to edge effects.

For a single time series of counts Y_t, hhh4 can be regarded as an extension of `glm.nb` from package **MASS** (Venables and Ripley 2002) to account for autoregression. See the `vignette("hhh4")` for examples of modeling univariate and bivariate count time series using hhh4. With multiple regions, spatio-temporal dependence is adopted by the third component in Equation 10 with weights w_{ji} reflecting the flow of infections from region j to region i. These transmission weights may be informed by movement network data (Paul *et al.* 2008; Schrödle *et al.* 2012; Geilhufe *et al.* 2014), but may also be estimated parametrically. A suitable choice to reflect epidemiological coupling between regions (Keeling and Rohani 2008, Chapter 7) is a power-law distance decay $w_{ji} = o_{ji}^{-d}$ defined in terms of the adjacency order o_{ji} in the neighbourhood graph of the regions (Meyer and Held 2014a). Note that we usually normalize the transmission weights such that $\sum_i w_{ji} = 1$, i.e., the $Y_{j,t-1}$ cases are distributed among the regions proportionally to the j'th row vector of the weight matrix (w_{ji}).

Likelihood inference for the above multivariate time-series model has been established by Paul and Held (2011) with extensions for parametric neighbourhood weights by Meyer and Held (2014a). Supplied with the analytical score function and Fisher information, the function hhh4 by default uses the quasi-Newton algorithm available through the R function `nlminb` to maximize the log-likelihood. Convergence is usually fast even for a large number of parameters. If the model contains random effects, the penalized and marginal log-likelihoods are maximized alternately until convergence. Computation of the marginal Fisher information is accelerated using the **Matrix** package (Bates and Maechler 2015).

5.2. Data structure: sts

We briefly introduce the S4-class sts used for data input in hhh4 models. See Höhle and Mazick (2010) and Salmon *et al.* (2015) for more detailed descriptions of this class, which is also used for the prospective aberration detection facilities of the **surveillance** package.

The epidemic modeling of multivariate count time series essentially involves three data matrices: a $T \times I$ matrix of the observed counts, a corresponding matrix with potentially time-varying population numbers (or fractions), and an $I \times I$ neighbourhood matrix quantifying the coupling between the I units. In our example, the latter consists of the adjacency orders o_{ji} between the districts. A map of the districts in the form of a `SpatialPolygons` object (defined by the **sp** package) can be used to derive the matrix of adjacency orders automatically using the functions `poly2adjmat` and `nbOrder`, which wrap functionality of package **spdep** (Bivand and Piras 2015):

```
R> weserems_nbOrder <- nbOrder(poly2adjmat(map), maxlag = 10)
```

Given the aforementioned ingredients, the sts object `data("measlesWeserEms")` included in **surveillance** has been constructed as follows:

```
R> measlesWeserEms <- sts(observed = counts, start = c(2001, 1), frequency = 52,
+    neighbourhood = weserems_nbOrder, map = map, population = populationFrac)
```

Here, `start` and `frequency` have the same meaning as for classical time-series objects of class `ts`, i.e., (year, sample number) of the first observation and the number of observa-

tions per year. Note that `data("measlesWeserEms")` constitutes a corrected version of `data("measles.weser")` originally used by Held *et al.* (2005).

We can visualize such `sts` data in four ways: individual time series, overall time series, map of accumulated counts by district, or animated maps. For instance, the two plots in Figure 13 have been generated by the following code:

```
R> plot(measlesWeserEms, type = observed ~ time)
R> plot(measlesWeserEms, type = observed ~ unit,
+    population = measlesWeserEms@map$POPULATION / 100000,
+    labels = list(font = 2), colorkey = list(space = "right"),
+    sp.layout = layout.scalebar(measlesWeserEms@map, corner = c(0.05, 0.05),
+      scale = 50, labels = c("0", "50 km"), height = 0.03))
```
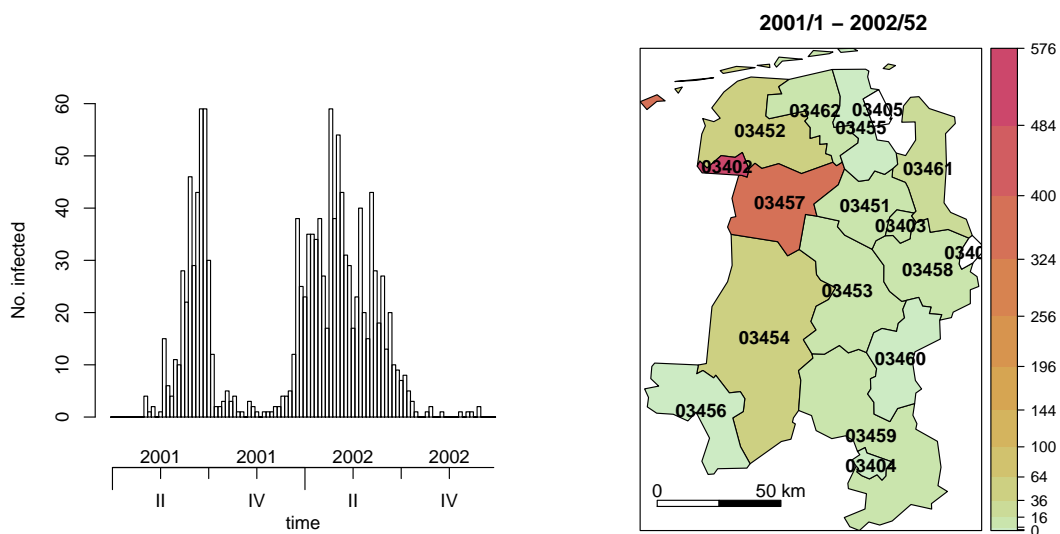

(a) Time series of weekly counts.   (b) Disease incidence (per 100 000 inhabitants).

Figure 13: Measles infections in the Weser-Ems region, 2001–2002.

The overall time-series plot in Figure 13a reveals strong seasonality in the data with slightly different patterns in the two years. The spatial plot in Figure 13b is a tweaked `spplot` (package **sp**) with colors from **colorspace** (Ihaka, Murrell, Hornik, Fisher, and Zeileis 2015) using $\sqrt{}$-equidistant cut points handled by package **scales** (Wickham 2015). The default plot `type` is `observed ~ time | unit` and shows the individual time series by district (Figure 14):

```
R> plot(measlesWeserEms, units = which(colSums(observed(measlesWeserEms)) > 0))
```

The plot excludes the districts 03401 (SK Delmenhorst) and 03405 (SK Wilhelmshaven) without any reported cases. Obviously, the districts have been affected by measles to a very heterogeneous extent during these two years.

An animation of the data can be easily produced as well. We recommend to use converters of the **animation** package, e.g., to watch the series of plots in a web browser. The following code will generate weekly disease maps during the year 2001 with the respective total number of cases shown in a legend and – if package **gridExtra** (Auguie 2015) is available – an evolving time-series plot at the bottom:
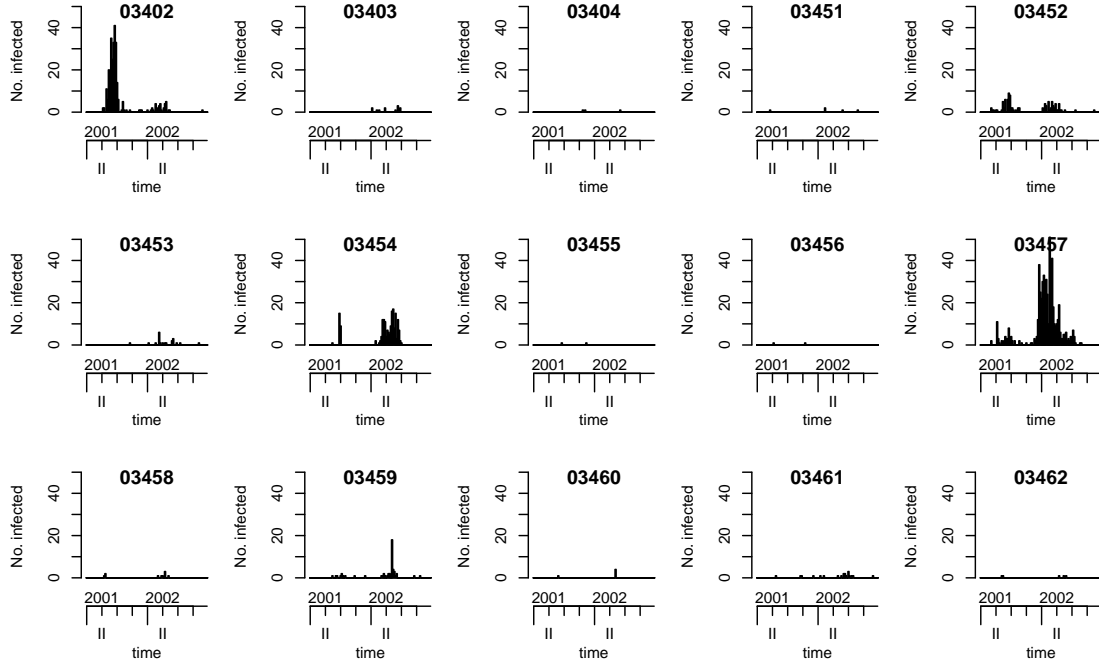
Figure 14: Count time series of the 15 affected districts.

```
R> animation::saveHTML(
+     animate(measlesWeserEms, tps = 1:52, total.args = list()),
+     title = "Evolution of the measles epidemic in the Weser-Ems region, 2001",
+     ani.width = 500, ani.height = 600)
```

5.3. Modeling and inference

For multivariate surveillance time series of counts such as the `measlesWeserEms` data, the function `hhh4` fits models of the form (10) via (penalized) maximum likelihood. We start by modeling the measles counts in the Weser-Ems region by a slightly simplified version of the original negative binomial model by Held *et al.* (2005). Instead of district-specific intercepts $\alpha_i^{(\nu)}$ in the endemic component, we first assume a common intercept $\alpha^{(\nu)}$ in order to not be forced to exclude the two districts without any reported cases of measles. After the estimation and illustration of this basic model, we will discuss the following sequential extensions: covariates (district-specific vaccination coverage), estimated transmission weights, and random effects to eventually account for unobserved heterogeneity of the districts.

Basic model

Our initial model has the following mean structure:

$$\mu_{it} = e_i\,\nu_t + \lambda\,Y_{i,t-1} + \phi \sum_{j \neq i} w_{ji} Y_{j,t-1} \,, \tag{14}$$

$$\log(\nu_t) = \alpha^{(\nu)} + \beta_t t + \gamma \sin(\omega t) + \delta \cos(\omega t) \,. \tag{15}$$

To account for temporal variation of disease incidence, the endemic log-linear predictor ν_t incorporates an overall trend and a sinusoidal wave of frequency $\omega = 2\pi/52$. As a basic district-specific measure of disease incidence, the population fraction e_i is included as a multiplicative offset. The epidemic parameters $\lambda = \exp(\alpha^{(\lambda)})$ and $\phi = \exp(\alpha^{(\phi)})$ are assumed homogeneous across districts and constant over time. Furthermore, we define $w_{ji} = \mathbb{1}(j \sim i) = \mathbb{1}(o_{ji} = 1)$ for the time being, which means that the epidemic can only arrive from directly adjacent districts. This `hhh4` model transforms into the following list of `control` arguments:

```
R> measlesModel_basic <- list(
+     end = list(f = addSeason2formula(~1 + t, period = measlesWeserEms@freq),
+                offset = population(measlesWeserEms)),
+     ar = list(f = ~1),
+     ne = list(f = ~1, weights = neighbourhood(measlesWeserEms) == 1),
+     family = "NegBin1")
```

The formulae of the three predictors $\log \nu_t$, $\log \lambda$ and $\log \phi$ are specified as element `f` of the `end`, `ar`, and `ne` lists, respectively. For the endemic formula we use the convenient function `addSeason2formula` to generate the sine-cosine terms, and we take the multiplicative `offset` of population fractions e_i from the `measlesWeserEms` object. The autoregressive part only consists of the intercept $\alpha^{(\lambda)}$, whereas the neighbourhood component specifies the intercept $\alpha^{(\phi)}$ and also the matrix of transmission `weights` (w_{ji}) to use – here a simple indicator of first-order adjacency. The chosen `family` corresponds to a negative binomial model with a common overdispersion parameter ψ for all districts. Alternatives are `"Poisson"`, `"NegBinM"` (ψ_i), or a factor determining which groups of districts share a common overdispersion parameter. Together with the data, the complete list of control arguments is then fed into the `hhh4` function to estimate the model, a summary of which is printed below.

```
R> measlesFit_basic <- hhh4(stsObj = measlesWeserEms, control = measlesModel_basic)
R> summary(measlesFit_basic, idx2Exp = TRUE, amplitudeShift = TRUE, maxEV = TRUE)

Call:
hhh4(stsObj = measlesWeserEms, control = measlesModel_basic)

Coefficients:
                       Estimate  Std. Error
exp(ar.1)               0.64540   0.07927
exp(ne.1)               0.01581   0.00420
exp(end.1)              1.08025   0.27884
exp(end.t)              1.00119   0.00426
end.A(2 * pi * t/52)    1.16423   0.19212
end.s(2 * pi * t/52)   -0.63436   0.13350
overdisp                2.01384   0.28544

Epidemic dominant eigenvalue:  0.72

Log-likelihood:    -972
AIC:               1957
BIC:               1996

Number of units:        17
Number of time points:  103
```

The `idx2Exp` argument requests the estimates for λ, ϕ, $\alpha^{(\nu)}$ and $\exp(\beta_t)$ instead of their respective internal log-values. For instance, `exp(end.t)` represents the seasonality-adjusted factor by which the basic endemic incidence increases per week. The `amplitudeShift` argument transforms the internal coefficients γ and δ of the sine-cosine terms to the amplitude A and phase shift φ of the corresponding sinusoidal wave $A\sin(\omega t + \varphi)$ in $\log \nu_t$ (Paul *et al.* 2008). The multiplicative effect of seasonality on ν_t is shown in Figure 15 produced by:

```
R> plot(measlesFit_basic, type = "season", components = "end", main = "")
```
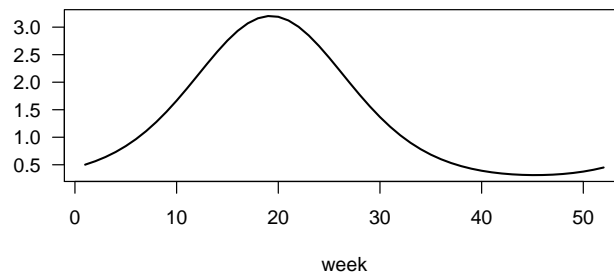

Figure 15: Estimated multiplicative effect of seasonality on the endemic mean.

The `overdisp` parameter and its 95% confidence interval obtained by

```
R> confint(measlesFit_basic, parm = "overdisp")


         2.5 % 97.5 %
overdisp  1.45   2.57
```

suggest that a negative binomial distribution with overdispersion is more adequate than a Poisson model corresponding to $\psi = 0$. We can underpin this finding by an AIC comparison, taking advantage of the convenient `update` method for `hhh4` fits:

```
R> AIC(measlesFit_basic, update(measlesFit_basic, family = "Poisson"))


                                         df  AIC
measlesFit_basic                          7 1957
update(measlesFit_basic, family = "Poisson")  6 2479
```

The epidemic potential of the process as determined by the parameters λ and ϕ is best investigated by a combined measure: the dominant eigenvalue (`maxEV`) of the matrix $\boldsymbol{\Lambda}$ which has the entries $(\Lambda)_{ii} = \lambda$ on the diagonal and $(\Lambda)_{ij} = \phi w_{ji}$ for $j \neq i$ (Paul *et al.* 2008). If the dominant eigenvalue is smaller than unity, it can be interpreted as the epidemic proportion of disease incidence. In the above model, the estimate is 72%. Another way of judging the relative importance of the three model components is to plot the fitted mean components along with the observed counts. Figure 16 shows this for the six districts with more than 20 cases:

```
R> districts2plot <- which(colSums(observed(measlesWeserEms)) > 20)
R> plot(measlesFit_basic, type = "fitted", units = districts2plot, hide0s = TRUE)
```
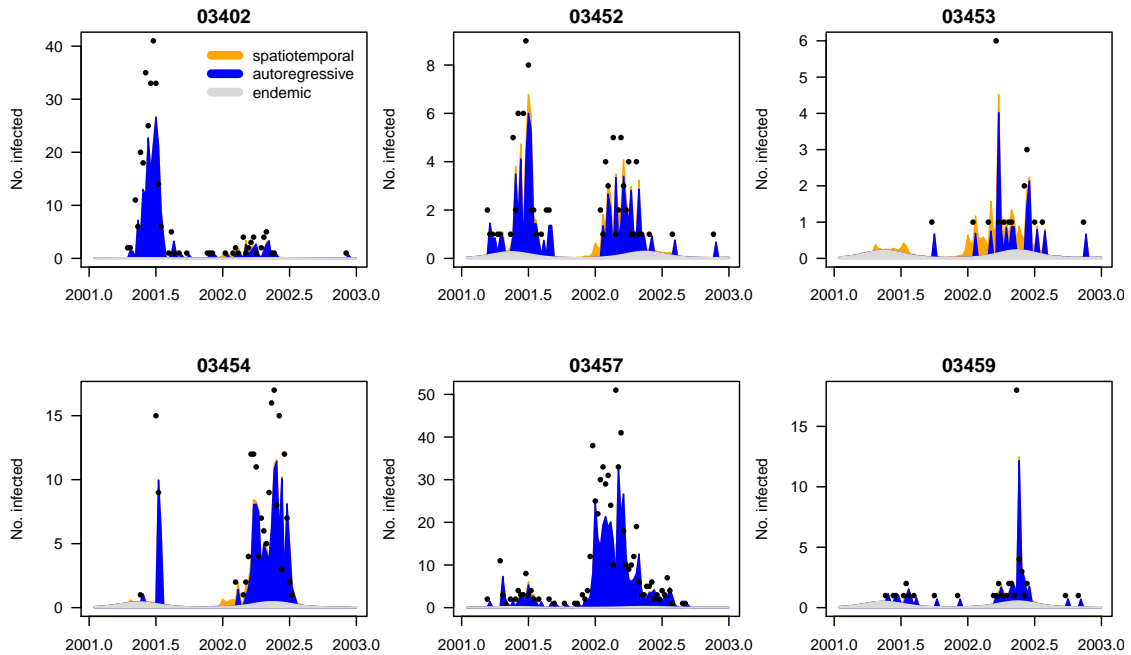
Figure 16: Fitted components in the initial model `measlesFit_basic` for the six districts with more than 20 cases. Dots are only drawn for positive weekly counts.

The largest portion of the fitted mean indeed results from the within-district autoregressive component with very little contribution of cases from adjacent districts and a rather small endemic incidence.

Other plot `types` and methods for fitted `hhh4` models as listed in Table 8 will be applied in the course of the following model extensions.

Covariates

The `hhh4` model framework allows for covariate effects on the endemic or epidemic contributions to disease incidence. Covariates may vary over both regions and time and thus obey the same $T \times I$ matrix structure as the observed counts. For infectious disease models, the regional vaccination coverage is an important example of such a covariate, since it reflects the (remaining) susceptible population. In a thorough analysis of measles occurrence in the German federal states, Herzog *et al.* (2011) found vaccination coverage to be associated with outbreak size. We follow their approach of using the district-specific proportion $1 - v_i$ of unvaccinated children just starting school as a proxy for the susceptible population. As v_i we use the proportion of children vaccinated with at least one dose among the ones presenting their vaccination card at school entry in district i in the year 2004.[5] This time-constant covariate needs to be transformed to the common matrix structure for incorporation in `hhh4`:

```
R> Sprop <- matrix(1 - measlesWeserEms@map@data$vacc1.2004,
+     nrow = nrow(measlesWeserEms), ncol = ncol(measlesWeserEms), byrow = TRUE)
```

---

[5]This is the first year with complete data for all 17 districts, available from the public health department of Lower Saxony at http://www.nlga.niedersachsen.de/portal/live.php?navigation_id=27093.

Display	Extract	Modify	Other
print	nobs	update	predict
summary	coef		simulate
plot	fixef		pit
	ranef		scores
	vcov		calibrationTest
	confint		all.equal
	coeflist		*oneStepAhead*
	logLik		
	residuals		
	terms		
	formula		

Table 8: Generic and *non-generic* functions applicable to `hhh4` objects.

```
R> summary(Sprop[1, ])
```

```
   Min. 1st Qu.  Median    Mean 3rd Qu.    Max.
 0.0306  0.0481  0.0581  0.0675  0.0830  0.1400
```

There are several ways to account for the susceptible proportion in our model, among which the simplest is to update the endemic population offset e_i by multiplication with $(1 - v_i)$. Herzog *et al.* (2011) found that the susceptible proportion is best added as a covariate in the autoregressive component in the form

$$\lambda_i \, Y_{i,t-1} = \exp\left(\alpha^{(\lambda)} + \beta_s \log(1 - v_i)\right) Y_{i,t-1} = \exp\left(\alpha^{(\lambda)}\right) (1 - v_i)^{\beta_s} \, Y_{i,t-1}$$

according to the mass action principle (Keeling and Rohani 2008). A higher proportion of susceptibles in district i is expected to boost the generation of new infections, i.e., $\beta_s > 0$. Alternatively, this effect could be assumed as an offset, i.e., $\beta_s \equiv 1$. To choose between endemic and/or autoregressive effects, and multiplicative offset vs. covariate modeling, we perform AIC-based model selection. First, we set up a grid of all combinations of envisaged extensions for the endemic and autoregressive components:

```
R> Soptions <- c("unchanged", "Soffset", "Scovar")
R> SmodelGrid <- expand.grid(end = Soptions, ar = Soptions)
R> row.names(SmodelGrid) <- do.call("paste", c(SmodelGrid, list(sep = "|")))
```

Then we update the initial model `measlesFit_basic` according to each row of `SmodelGrid`:

```
R> measlesFits_vacc <- apply(X = SmodelGrid, MARGIN = 1, FUN = function (options) {
+    updatecomp <- function (comp, option) switch(option,
+      "unchanged" = list(),
+      "Soffset" = list(offset = comp$offset * Sprop),
+      "Scovar" = list(f = update(comp$f, ~. + log(Sprop))))
+    update(measlesFit_basic,
+      end = updatecomp(measlesFit_basic$control$end, options[1]),
+      ar = updatecomp(measlesFit_basic$control$ar, options[2]),
+      data = list(Sprop = Sprop))
+    })
```

The resulting object `measlesFits_vacc` is a list of 9 `hhh4` fits, which are named according to the corresponding `Soptions` used for the endemic and autoregressive component. We construct a call of the function `AIC` taking all list elements as arguments:

```
R> aics_vacc <- do.call(AIC, lapply(names(measlesFits_vacc), as.name),
+     envir = as.environment(measlesFits_vacc))
R> aics_vacc[order(aics_vacc[, "AIC"]), ]
```

```
                     df  AIC
`Scovar|unchanged`    8 1917
`Scovar|Scovar`       9 1919
`Soffset|unchanged`   7 1922
`Soffset|Scovar`      8 1924
`Scovar|Soffset`      8 1934
`Soffset|Soffset`     7 1937
unchanged|unchanged   7 1957
`unchanged|Scovar`    8 1959
`unchanged|Soffset`   7 1967
```

Hence, AIC increases if the susceptible proportion is only added to the autoregressive component, but we see a remarkable improvement when adding it to the endemic component. The best model is obtained by leaving the autoregressive component unchanged (λ) and adding the term $\beta_s \log(1 - v_i)$ to the endemic predictor in Equation 15.

```
R> measlesFit_vacc <- measlesFits_vacc[["Scovar|unchanged"]]
R> coef(measlesFit_vacc, se = TRUE)["end.log(Sprop)", ]
```

```
  Estimate Std. Error
     1.718      0.288
```

The estimated exponent $\hat{\beta}_s$ is both clearly positive and different from the offset assumption. In other words, if a district's fraction of susceptibles is doubled, the endemic measles incidence is estimated to multiply by $2^{\hat{\beta}_s} = 3.29$ (95% CI: 2.23–4.86).

Spatial interaction

Up to now, the model assumed that the epidemic can only arrive from directly adjacent districts because $w_{ji} = \mathbb{1}(j \sim i)$, and that all districts have the same potential ϕ for importing cases from neighbouring regions. Given the ability of humans to travel further and preferrably to metropolitan areas, both assumptions seem overly simplistic. First, to reflect commuter-driven spread in our model, we scale the district's susceptibility according to its population fraction by multiplying ϕ by $e_i^{\beta_{pop}}$:

```
R> measlesFit_nepop <- update(measlesFit_vacc,
+     ne = list(f = ~log(pop)), data = list(pop = population(measlesWeserEms)))
```

As in a similar analysis of influenza (Meyer and Held 2014a), we find strong evidence for such an agglomeration effect: the estimated exponent is $\hat{\beta}_{pop} = 2.85$ (95% CI: 1.83–3.87) and AIC decreases from 1917 to 1887. Models where attraction to a region scales with population size are called "gravity" models (Xia, Bjørnstad, and Grenfell 2004).
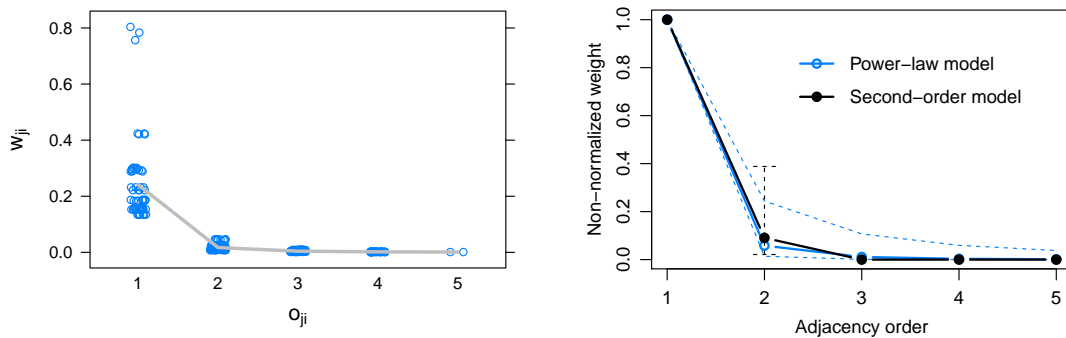
(a) Normalized weights in the power-law model.   (b) Non-normalized weights with 95% CIs.

Figure 17: Estimated weights as a function of adjacency order.

To account for long-range transmission of cases, Meyer and Held (2014a) proposed to estimate the weights w_{ji} as a function of the adjacency order o_{ji} between the districts. For instance, a power-law model assumes the form $w_{ji} = o_{ji}^{-d}$, for $j \neq i$ and $w_{jj} = 0$, where the decay parameter d is to be estimated. Normalization to $w_{ji} / \sum_k w_{jk}$ is recommended and applied by default when supplying `W_powerlaw` as weights in the neighbourhood component:

```
R> measlesFit_powerlaw <- update(measlesFit_nepop,
+    ne = list(weights = W_powerlaw(maxlag = 5)))
```

The argument `maxlag` sets an upper bound for spatial interaction in terms of adjacency order. Here we set no limit since `max(neighbourhood(measlesWeserEms))` is 5. The resulting parameter estimate is $\hat{d} = 4.10$ (95% CI: 2.03–6.17), which represents a strong decay of spatial interaction for higher-order neighbours. As an alternative to the parametric power law, unconstrained weights up to `maxlag` can be estimated by using `W_np` instead of `W_powerlaw`. For instance, `W_np(maxlag = 2)` corresponds to a second-order model, i.e., $w_{ji} = 1 \cdot \mathbb{1}(o_{ji} = 1) + e^{\omega_2} \cdot \mathbb{1}(o_{ji} = 2)$, which is also row-normalized by default:

```
R> measlesFit_np2 <- update(measlesFit_nepop,
+    ne = list(weights = W_np(maxlag = 2)))
```

Figure 17b shows both the power law model $o^{-\hat{d}}$ and the second-order model, where $e^{\hat{\omega}_2} = 0.09$ (95% CI: 0.02–0.39). Alternatively, the plot `type = "neweights"` for `hhh4` fits can produce a `stripplot` (Sarkar 2008) of w_{ji} against o_{ji} as shown in Figure 17a for the power-law model:

```
R> library("lattice")
R> plot(measlesFit_powerlaw, type = "neweights", plotter = stripplot,
+    panel = function (...) {panel.stripplot(...); panel.average(...)},
+    jitter.data = TRUE, xlab = expression(o[ji]), ylab = expression(w[ji]))
```

Note that only horizontal jitter is added in this case. Because of normalization, the weight w_{ji} for transmission from district j to district i is determined not only by the districts' neighbourhood o_{ji} but also by the total amount of neighbourhood of district j in the form of $\sum_{k \neq j} o_{jk}^{-d}$, which causes some variation of the weights for a specific order of adjacency.

An AIC comparison of the different models for the transmission weights yields:

```
R> AIC(measlesFit_nepop, measlesFit_powerlaw, measlesFit_np2)
```

```
                     df  AIC
measlesFit_nepop      9 1887
measlesFit_powerlaw  10 1882
measlesFit_np2       10 1881
```

AIC improves when accounting for transmission between higher-order neighbours by a power law or a second-order model. In spite of the latter resulting in a slightly better fit, we will use the power-law model as a basis for further model extensions since the stand-alone second-order effect is not always identifiable in more complex models and is scientifically implausible.

Random effects

[Paul and Held](2011) introduced random effects for `hhh4` models, which are useful if the districts exhibit heterogeneous incidence levels not explained by observed covariates, and especially if the number of districts is large. For infectious disease surveillance data, a typical example of unobserved heterogeneity is under-reporting ([Bernard, Werber, and Höhle 2014](#)). Our measles data even contain two districts without any reported cases, while the district with the smallest population (03402, SK Emden) had the second-largest number of cases reported and the highest overall incidence (see Figures [13b](#) and [14](#)). Hence, allowing for district-specific intercepts in the endemic or epidemic components is expected to improve the model fit. For independent random effects $\alpha_i^{(\nu)} \overset{iid}{\sim} \mathrm{N}(\alpha^{(\nu)}, \sigma_\nu^2)$, $\alpha_i^{(\lambda)} \overset{iid}{\sim} \mathrm{N}(\alpha^{(\lambda)}, \sigma_\lambda^2)$, and $\alpha_i^{(\phi)} \overset{iid}{\sim} \mathrm{N}(\alpha^{(\phi)}, \sigma_\phi^2)$ in all three components, we update the corresponding formulae as follows:

```
R> measlesFit_ri <- update(measlesFit_powerlaw,
+    end = list(f = update(formula(measlesFit_powerlaw)$end, ~. + ri() - 1)),
+    ar  = list(f = update(formula(measlesFit_powerlaw)$ar,  ~. + ri() - 1)),
+    ne  = list(f = update(formula(measlesFit_powerlaw)$ne,  ~. + ri() - 1)))
```

```
R> summary(measlesFit_ri, amplitudeShift = TRUE, maxEV = TRUE)
```

```
Call:
hhh4(stsObj = object$stsObj, control = control)

Random effects:
            Var    Corr
ar.ri(iid)  1.076
ne.ri(iid)  1.294 0
end.ri(iid) 1.312 0    0

Fixed effects:
                   Estimate  Std. Error
ar.ri(iid)         -1.61389  0.38197
ne.log(pop)         3.42406  1.07722
ne.ri(iid)          6.62429  2.81553
end.t               0.00578  0.00480
end.A(2 * pi * t/52) 1.20359  0.20149
end.s(2 * pi * t/52) -0.47916  0.14205
end.log(Sprop)      1.79350  0.69159
```

```
end.ri(iid)          4.42260   1.94605
neweights.d          3.60640   0.77602
overdisp             0.97723   0.15132


Epidemic dominant eigenvalue:  0.84


Penalized log-likelihood:  -869
Marginal log-likelihood:   -54.2


Number of units:         17
Number of time points:  103
```

The summary now contains an extra section with the estimated variance components σ_λ^2, σ_ϕ^2, and σ_ν^2 of the random effects. We did not assume correlation between the three intercepts, but this is possible by specifying `ri(corr = "all")` in the component formulae. The implementation also supports a conditional autoregressive formulation (Besag, York, and Mollié 1991) for spatially correlated intercepts by using `ri(type = "car")`. The estimated district-specific intercepts can be extracted by the `ranef`-method:

```
R> head(ranef(measlesFit_ri, tomatrix = TRUE), n = 3)


      ar.ri(iid) ne.ri(iid) end.ri(iid)
03401      0.000    -0.0567       -1.00
03402      1.223     0.0431        1.53
03403     -0.827     1.5588       -0.62
```

They can also be visualized in a map by the plot `type = "ri"`:

```
R> for (comp in c("ar", "ne", "end")) {
+    print(plot(measlesFit_ri, type = "ri", component = comp,
+      col.regions = rev(cm.colors(100)), labels = list(cex = 0.6),
+      at = seq(-1.6, 1.6, length.out = 15)))
+ }
```


(a) Autoregressive $\alpha_i^{(\lambda)}$ (b) Spatio-temporal $\alpha_i^{(\phi)}$ (c) Endemic $\alpha_i^{(\nu)}$
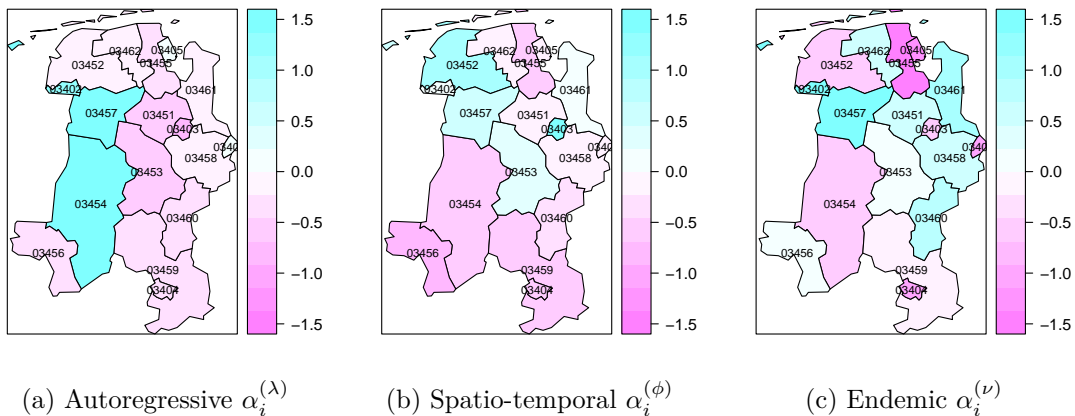
Figure 18: Maps of the estimated random intercepts.

For the autoregressive component in Figure 18a, we see a pronounced heterogeneity between the three western districts in blue and the remaining districts. These three districts have been affected by large local outbreaks and are also the ones with the highest overall numbers of cases. In contrast, the city of Oldenburg (03403) is estimated with a relatively low autoregressive factor $\lambda_i = \exp(\alpha^{(\lambda)} + \alpha_i^{(\lambda)}) = 0.087$, but it seems to import more cases from other districts than explained by its population (Figure 18b). In Figure 18c, the two districts without any reported measles cases (03401 and 03405) appear in dark pink, which means that they exhibit a relatively low endemic incidence after adjusting for the population and susceptible proportion. Such districts could be suspected of a larger amount of under-reporting.

Note that the extra flexiblility of the random effects model comes at a price. First, the estimation runtime increases considerably from 0.1 seconds for the previous power-law model `measlesFit_powerlaw` to 4 seconds with additional random effects. Furthermore, we no longer obtain AIC values in the model summary, since random effects invalidate simple AIC-based model comparisons (Greven and Kneib 2010). Of course we can plot the fitted values and visually compare their quality with the initial fit shown in Figure 16:

```
R> plot(measlesFit_ri, type = "fitted", units = districts2plot, hide0s = TRUE)
```
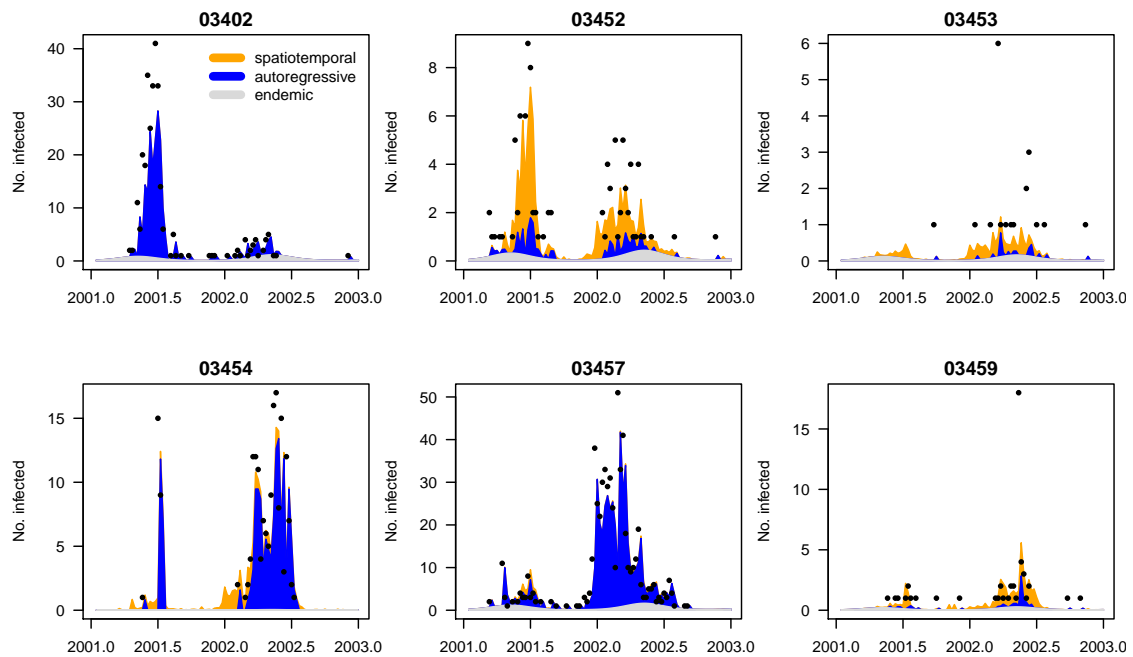

Figure 19: Fitted components in the random effects model `measlesFit_ri` for the six districts with more than 20 cases. Compare to Figure 16.

For some of these districts, a great amount of cases is now explained via transmission from neighbouring regions while others are mainly influenced by the local autoregression. Note that the estimated decomposition of the mean by district can also be seen from the related plot `type = "maps"` (not shown). However, for quantitative comparisons of model performance we have to resort to more sophisticated techniques presented in the next section.

Predictive model assessment

Paul and Held (2011) suggest to evaluate one-step-ahead forecasts from competing models by proper scoring rules for count data (Czado, Gneiting, and Held 2009). These scores measure the discrepancy between the predictive distribution P from a fitted model and the later observed value y. A well-known example is the squared error score ("ses") $(y - \mu_P)^2$, which is usually averaged over a suitable set of forecasts to obtain the mean squared error. More elaborate scoring rules such as the logarithmic score ("logs") or the ranked probability score ("rps") take into account the whole predictive distribution to assess calibration and sharpness simultaneously – see the recent review by Gneiting and Katzfuss (2014). The so-called Dawid-Sebastiani score ("dss") is another option. Lower scores correspond to better predictions.

In the `hhh4` framework, predictive model assessment is made available by the functions `oneStepAhead`, `scores`, `pit`, and `calibrationTest`. We will use the second quarter of 2002 as the test period, and compare the basic model, the power-law model, and the random effects model. First, we use the `"final"` fits on the complete time series to compute the predictions, which then simply correspond to the fitted values during the test period:

```
R> tp <- c(65, 77)
R> models2compare <- paste0("measlesFit_", c("basic", "powerlaw", "ri"))
R> measlesPreds1 <- lapply(mget(models2compare), oneStepAhead,
+    tp = tp, type = "final")
```

Note that in this case, the log-score for a model's prediction in district i in week t equals the associated negative log-likelihood contribution. Comparing the mean scores from different models is thus essentially a goodness-of-fit assessment:

```
R> SCORES <- c("logs", "rps", "dss", "ses")
R> measlesScores1 <- lapply(measlesPreds1, scores, which = SCORES, individual = TRUE)
R> t(sapply(measlesScores1, colMeans, dims = 2))
```

```
                   logs   rps   dss  ses
measlesFit_basic    1.09 0.736 1.291 5.29
measlesFit_powerlaw 1.10 0.731 2.222 5.39
measlesFit_ri       1.01 0.638 0.966 4.82
```

All scoring rules claim that the random effects model gives the best fit during the second quarter of 2002. Now we turn to true one-week-ahead predictions of `type = "rolling"`, which means that we always refit the model up to week t to get predictions for week $t + 1$:

```
R> measlesPreds2 <- lapply(mget(models2compare), oneStepAhead,
+    tp = tp, type = "rolling", which.start = "final",
+    cores = 2 * (.Platform$OS.type == "unix"))
R> measlesScores2 <- lapply(measlesPreds2, scores, which = SCORES, individual = TRUE)
R> t(sapply(measlesScores2, colMeans, dims = 2))
```

```
                   logs   rps   dss  ses
measlesFit_basic    1.10 0.748 1.34 5.40
measlesFit_powerlaw 1.14 0.765 2.93 5.87
measlesFit_ri       1.11 0.763 2.35 7.08
```

Thus, the most parsimonious initial model `measlesFit_basic` gives the best one-week-ahead predictions in terms of overall mean scores. Statistical significance of the differences in mean scores can be investigated by a `permutationTest` for paired data or a paired t-test:

```
R> set.seed(321)
R> sapply(SCORES, function (score) permutationTest(
+     measlesScores2$measlesFit_ri[, , score],
+     measlesScores2$measlesFit_basic[, , score]))


             logs    rps    dss   ses
diffObs      0.00782 0.0154 1.01  1.68
pVal.permut  0.867   0.72   0.518 0.19
pVal.t       0.854   0.717  0.374 0.171
```

Hence, there is no clear evidence for a difference between the basic and the random effects model with regard to predictive performance during the test period. Whether predictions of a particular model are well calibrated can be formally investigated by `calibrationTest`s for count data as recently proposed by (Wei and Held 2014). For example:

```
R> calibrationTest(measlesPreds2[["measlesFit_ri"]], which = "rps")


Calibration Test for Count Data (based on RPS)

data:  measlesPreds2[["measlesFit_ri"]]
z = 0.80671, n = 221, p-value = 0.4198
```

Thus, there is no evidence of miscalibrated predictions from the random effects model. Czado *et al.* (2009) describe an alternative informal approach to assess calibration: probability integral transform (PIT) histograms for count data (Figure 20).

```
R> for (m in models2compare)
+     pit(measlesPreds2[[m]], plot = list(ylim = c(0, 1.25), main = m))
```
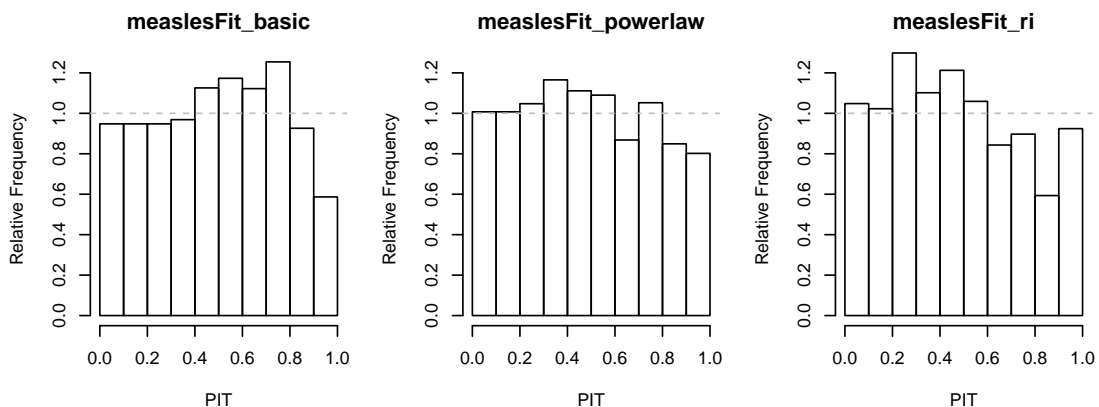

Figure 20: PIT histograms of competing models to check calibration of the one-week-ahead predictions during the second quarter of 2002.

Under the hypothesis of calibration, i.e., $y_{it} \sim P_{it}$ for all predictive distributions P_{it} in the test period, the PIT histogram is uniform. Underdispersed predictions lead to U-shaped histograms, and bias causes skewness. In this aggregate view of the predictions over all districts and weeks of the test period, predictive performance is comparable between the models, and there is no evidence of badly dispersed predictions. However, the right-hand decay in all histograms suggests that all models tend to predict higher counts than observed. This is most likely related to the seasonal shift between the years 2001 and 2002. In 2001, the peak of the epidemic was in the second quarter, while it already occured in the first quarter in 2002 (cp. Figure 13a).

Further modeling options

In the previous sections we extended our model for measles in the Weser-Ems region with respect to spatial variation of the counts and their interaction. Temporal variation was only accounted for in the endemic component, which included a long-term trend and a sinusoidal wave on the log-scale. Held and Paul (2012) suggest to also allow seasonal variation of the epidemic force by adding a superposition of S harmonic waves of fundamental frequency ω, $\sum_{s=1}^{S} \{\gamma_s \sin(s\,\omega t) + \delta_s \cos(s\,\omega t)\}$, to the log-linear predictors of the autoregressive and/or neighbourhood component – just like for $\log \nu_t$ in Equation 15 with $S = 1$. However, given only two years of measles surveillance and the apparent shift of seasonality with regard to the start of the outbreak in 2002 compared to 2001, more complex seasonal models are likely to overfit the data. Concerning the coding in R, sine-cosine terms can be added to the epidemic components without difficulties by again using the convenient function `addSeason2formula`. Updating a previous model for different numbers of harmonics is even simpler, since the `update`-method has a corresponding argument S. The plots of `type = "season"` and `type = "maxEV"` for `hhh4` fits can visualize the estimated component seasonality.

All of our models for the measles surveillance data incorporated an epidemic effect of the counts from the local district and its neighbours. Without further notice, we thereby assumed a lag equal to the observation interval of one week. However, the generation time of measles is around 10 days (Anderson and May 1991), which is why some studies, e.g., Finkenstädt, Bjørnstad, and Grenfell (2002) or Herzog *et al.* (2011), aggregate their weekly measles surveillance data into biweekly intervals. Fine and Clarkson (1982) used weekly counts in their analysis and report that biweekly aggregation would have little effect on the results. We can also perform such a sensitivity analysis by running the whole code of the current section based on `aggregate(measlesWeserEms, nfreq = 26)`. Doing so, the parameter estimates of the various models retain their order of magnitude and conclusions remain the same. However, with the number of time points halved, the complex random effects model would not always be identifiable when calculating one-week-ahead predictions during the test period.

We have shown several options to account for the spatio-temporal dynamics of infectious disease spread. However, for directly transmitted human diseases, the social phenomenon of "like seeks like" results in contact patterns between subgroups of a population, which extend the pure distance decay of interaction. Especially for school children, social contacts are known to be highly assortative with respect to age (Mossong *et al.* 2008). A useful epidemic model should therefore be additionally stratified by age group and take the inherent contact structure into account. How this extension can be incorporated in the spatio-temporal endemic-epidemic modeling framework `hhh4` is the focus of current research.

5.4. Simulation

Simulation from fitted `hhh4` models is enabled by an associated `simulate`-method. Compared to the point process models of Sections 3 and 4, simulation is less complex since it essentially consists of sequential calls of `rnbinom` (or `rpois`). At each time point t, the mean μ_{it} is determined by plugging in the parameter estimates and the counts $Y_{i,t-1}$ simulated at the previous time point. In addition to a model fit, we thus need to specify an initial vector of counts `y.start`. As an example, we simulate 100 realizations of the evolution of measles during the year 2002 based on the fitted random effects model and the counts of the last week of the year 2001 in the 17 districts:

```
R> (y.start <- observed(measlesWeserEms)[52, ])
```

```
03401 03402 03403 03404 03405 03451 03452 03453 03454 03455 03456 03457 03458 03459
    0     0     0     0     0     0     0     0     0     0     0    25     0     0
03460 03461 03462
    0     0     0
```

```
R> measlesSim <- simulate(measlesFit_ri,
+    nsim = 100, seed = 1, subset = 53:104, y.start = y.start)
```

The simulated counts are returned as a $52 \times 17 \times 100$ array instead of a list of 100 `sts` objects. We can, e.g., look at the final size distribution of the simulations:

```
R> summary(colSums(measlesSim, dims = 2))
```

```
  Min. 1st Qu.  Median    Mean 3rd Qu.    Max.
   223     326     424     550     582    3970
```

A few large outbreaks have been simulated, but the mean size is below the observed number of `sum(observed(measlesWeserEms)[53:104, ])` = 779 cases in the year 2002. Using the `plot`-method associated with such `hhh4` simulations, Figure 21 shows the weekly number of observed cases compared to the long-term forecast:

```
R> plot(measlesSim, "time", ylim = c(0, 100))
```

We refer to `help("simulate.hhh4")` for further examples.

6. Conclusion

In the present work we have introduced the R package **surveillance** as a comprehensive statistical framework for the analysis of spatio-temporal surveillance data covering individual-level event data as well as aggregated count data time series. The package offers a multitude of methods for visualization, likelihood inference and simulation of endemic-epidemic models. Additional functionality beyond the illustrations in Sections 3 to 5 can be found via `help(package = "surveillance")`. By the open-source implementation of recently developed statistical methodology in a readily available R package, we support reproducibility of research and hope to serve an increased need in analyzing spatio-temporal epidemic data using statistical models.
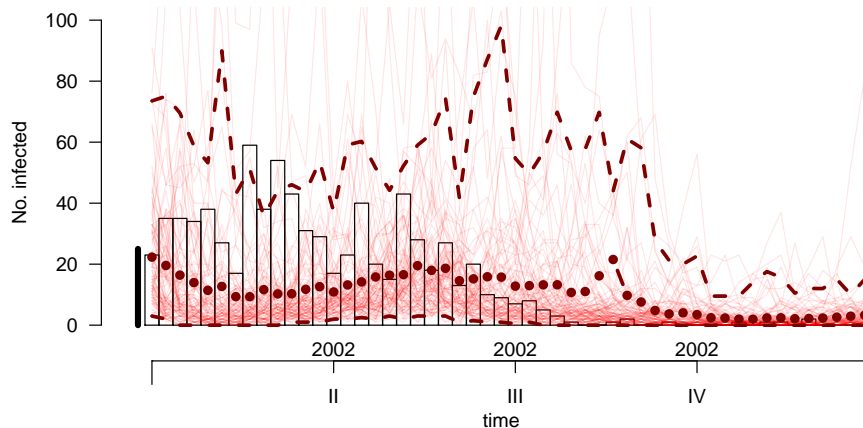
Figure 21: Simulation-based long-term forecast starting from the last week in 2001 (vertical bar on the left), showing the counts aggregated over all districts. The weekly mean of the simulations is represented by dots and the dashed lines correspond to the pointwise 2.5% and 97.5% quantiles. The actually observed counts are shown in the background.

Acknowledgements

Involved **R** packages and versions

This paper is based on **surveillance** 1.10-0 (Höhle, Meyer, and Paul 2015) in R version 3.2.2 (2015-08-14) using **knitr** (Xie 2015) for dynamic report generation. The implementations of the three presented endemic-epidemic modeling frameworks rely on several other R packages. In the following we list all packages involved as first-order dependencies of **surveillance** with the versions used in this paper: **sp** 1.2-1 (Pebesma and Bivand 2005), **xtable** 1.8-0 (Dahl 2015), **polyCub** 0.5-2 (Meyer 2015), **MASS** 7.3-44 (Venables and Ripley 2002), **Matrix** 1.2-2 (Bates and Maechler 2015), **spatstat** 1.43-0 (Baddeley *et al.* 2015), **lattice** 0.20-33 (Sarkar 2008), **colorspace** 1.2-6 (Ihaka *et al.* 2015), **scales** 0.3.0 (Wickham 2015), **quadprog** 1.5-5 (Turlach 2013), **memoise** 0.2.1 (Wickham 2014), **polyclip** 1.3-2 (Johnson 2015), **maptools** 0.8-

37 (Bivand and Lewin-Koh 2015) and **spdep** 0.5-88 (Bivand and Piras 2015).

R itself, the **surveillance** package, and all other aforementioned packages are available from the Comprehensive R Archive Network (CRAN) at `https://CRAN.R-project.org/`. The development of **surveillance** is hosted at `http://surveillance.r-forge.r-project.org/`.

References

Adelfio G, Chiodi M (2015). "FLP Estimation of Semi-parametric Models for Space–time Point Processes and Diagnostic Tools." *Spatial Statistics*. ISSN 2211-6753. `doi:10.1016/j.spasta.2015.06.004`. In press.

Anderson RM, May RM (1991). *Infectious Diseases of Humans: Dynamics and Control*. Oxford University Press.

Auguie B (2015). **gridExtra**: *Miscellaneous Functions for "Grid" Graphics*. R package version 2.0.0, URL `http://CRAN.R-project.org/package=gridExtra`.

Baddeley A, Rubak E, Turner R (2015). *Spatial Point Patterns: Methodology and Applications with R*. Chapman and Hall/CRC Press, London. In press, URL `http://www.crcpress.com/Spatial-Point-Patterns-Methodology-and-Applications-with-R/Baddeley-Rubak-Turner/9781482210200/`.

Balderama E, Schoenberg FP, Murray E, Rundel PW (2012). "Application of Branching Models in the Study of Invasive Species." *Journal of the American Statistical Association*, **107**(498), 467–476. `doi:10.1080/01621459.2011.641402`.

Bates D, Maechler M (2015). **Matrix**: *Sparse and Dense Matrix Classes and Methods*. R package version 1.2-2, URL `http://CRAN.R-project.org/package=Matrix`.

Bernard H, Werber D, Höhle M (2014). "Estimating the Under-Reporting of Norovirus Illness in Germany Utilizing Enhanced Awareness of Diarrhoea During a Large Outbreak of Shiga Toxin-Producing E. Coli O104:H4 in 2011 – A Time Series Analysis." *BMC Infectious Diseases*, **14**(1), 116. `doi:10.1186/1471-2334-14-116`.

Besag J, York J, Mollié A (1991). "Bayesian Image-Restoration, with Two Applications in Spatial Statistics." *The Annals of the Institute of Statistical Mathematics*, **43**(1), 1–20.

Bivand R, Keitt T, Rowlingson B (2015). **rgdal**: *Bindings for the Geospatial Data Abstraction Library*. R package version 1.1-1, URL `http://CRAN.R-project.org/package=rgdal`.

Bivand R, Lewin-Koh N (2015). **maptools**: *Tools for Reading and Handling Spatial Objects*. R package version 0.8-37, URL `http://CRAN.R-project.org/package=maptools`.

Bivand R, Piras G (2015). "Comparing Implementations of Estimation Methods for Spatial Econometrics." *Journal of Statistical Software*, **63**(18), 1–36. URL `http://www.jstatsoft.org/v63/i18/`.

Bivand RS, Pebesma E, Gómez-Rubio V (2013). *Applied Spatial Data Analysis with R*, volume 10 of *Use R!* 2nd edition. Springer-Verlag, New York. ISBN 1-4614-7617-8. URL `http://www.asdar-book.org`.

Brown PE (2015). "Model-Based Geostatistics the Easy Way." *Journal of Statistical Software*, **63**(12), 1–24. ISSN 1548-7660. URL http://www.jstatsoft.org/v63/i12.

Cori A, Ferguson NM, Fraser C, Cauchemez S (2013). "A New Framework and Software to Estimate Time-Varying Reproduction Numbers During Epidemics." *American Journal of Epidemiology*, **178**(9), 1505–1512. doi:10.1093/aje/kwt133.

Czado C, Gneiting T, Held L (2009). "Predictive Model Assessment for Count Data." *Biometrics*, **65**(4), 1254–1261. doi:10.1111/j.1541-0420.2009.01191.x.

Dahl DB (2015). **xtable**: *Export Tables to LaTeX or HTML*. R package version 1.8-0, URL http://CRAN.R-project.org/package=xtable.

Daley DJ, Gani J (1999). *Epidemic Modelling: An Introduction*, volume 15 of *Cambridge Studies in Mathematical Biology*. Cambridge University Press. ISBN 0-521-64079-2. doi:10.1017/CBO9780511608834.

Daley DJ, Vere-Jones D (2003). *An Introduction to the Theory of Point Processes*, volume I: Elementary Theory and Methods of *Probability and its Applications*. 2nd edition. Springer-Verlag, New York. ISBN 0-387-95541-0.

Diggle PJ (2006). "Spatio-Temporal Point Processes, Partial Likelihood, Foot and Mouth Disease." *Statistical Methods in Medical Research*, **15**(4), 325–336. doi:10.1191/0962280206sm454oa.

Douglas DH, Peucker TK (1973). "Algorithms for the Reduction of the Number of Points Required to Represent a Digitized Line or its Caricature." *Cartographica: The International Journal for Geographic Information and Geovisualization*, **10**(2), 112–122. doi:10.3138/FM57-6770-U75U-7727.

Fahrmeir L, Kneib T, Lang S, Marx B (2013). *Regression: Models, Methods and Applications*. Springer-Verlag. ISBN 3-642-34332-5. doi:10.1007/978-3-642-34333-9.

Fine PEM, Clarkson JA (1982). "Measles in England and Wales—I: An Analysis of Factors Underlying Seasonal Patterns." *International Journal of Epidemiology*, **11**(1), 5–14. doi:10.1093/ije/11.1.5.

Finkenstädt BF, Bjørnstad ON, Grenfell BT (2002). "A Stochastic Model for Extinction and Recurrence of Epidemics: Estimation and Inference for Measles Outbreaks." *Biostatistics*, **3**(4), 493–510. doi:10.1093/biostatistics/3.4.493.

Finkenstädt BF, Grenfell BT (2000). "Time Series Modelling of Childhood Diseases: A Dynamical Systems Approach." *Journal of the Royal Statistical Society C*, **49**(2), 187–205. doi:10.1111/1467-9876.00187.

Geilhufe M, Held L, Skrøvseth SO, Simonsen GS, Godtliebsen F (2014). "Power Law Approximations of Movement Network Data for Modeling Infectious Disease Spread." *Biometrical Journal*, **56**(3), 363–382. doi:10.1002/bimj.201200262.

Gneiting T, Katzfuss M (2014). "Probabilistic Forecasting." *Annual Review of Statistics and Its Application*, **1**(1), 125–151. doi:10.1146/annurev-statistics-062713-085831.

Greven S, Kneib T (2010). "On the Behaviour of Marginal and Conditional AIC in Linear Mixed Models." *Biometrika*, **97**(4), 773–789. `doi:10.1093/biomet/asq042`.

Groendyke C, Welch D, Hunter DR (2012). "A Network-Based Analysis of the 1861 Hagelloch Measles Data." *Biometrics*, **68**(3), 755–765. `doi:10.1111/j.1541-0420.2012.01748.x`.

Harrower M, Bloch M (2006). "Mapshaper.org: A Map Generalization Web Service." *IEEE Computer Graphics and Applications*, **26**(4), 22–27. `doi:10.1109/MCG.2006.85`.

Held L, Hofmann M, Höhle M, Schmid V (2006). "A Two-Component Model for Counts of Infectious Diseases." *Biostatistics*, **7**(3), 422–437. `doi:10.1093/biostatistics/kxj016`.

Held L, Höhle M, Hofmann M (2005). "A Statistical Framework for the Analysis of Multivariate Infectious Disease Surveillance Counts." *Statistical Modelling*, **5**(3), 187–199. `doi:10.1191/1471082X05st098oa`.

Held L, Paul M (2012). "Modeling Seasonality in Space-Time Infectious Disease Surveillance Data." *Biometrical Journal*, **54**(6), 824–843. `doi:10.1002/bimj.201200037`.

Herzog SA, Paul M, Held L (2011). "Heterogeneity in Vaccination Coverage Explains the Size and Occurrence of Measles Epidemics in German Surveillance Data." *Epidemiology and Infection*, **139**(04), 505–515. `doi:10.1017/S0950268810001664`.

Hughes AW, King ML (2003). "Model Selection Using AIC in the Presence of One-Sided Information." *Journal of Statistical Planning and Inference*, **115**(2), 397–411. `doi:10.1016/S0378-3758(02)00159-3`.

Höhle M (2007). "**surveillance**: An R package for the monitoring of infectious diseases." *Computational Statistics*, **22**(4), 571–582. `doi:10.1007/s00180-007-0074-8`.

Höhle M (2009). "Additive-Multiplicative Regression Models for Spatio-Temporal Epidemics." *Biometrical Journal*, **51**(6), 961–978. `doi:10.1002/bimj.200900050`.

Höhle M (2016). "Infectious Disease Modelling." In AB Lawson, S Banerjee, RP Haining, MD Ugarte (eds.), *Handbook of Spatial Epidemiology*, Chapman & Hall/CRC Handbooks of Modern Statistical Methods. Chapman and Hall/CRC. ISBN 1-4822-5301-1. Forthcoming, `http://www.math.su.se/~hoehle/pubs/Hoehle_SpaMethInfEpiModelling2015.pdf`.

Höhle M, Mazick A (2010). "Aberration Detection in R Illustrated by Danish Mortality Monitoring." In TA Kass-Hout, X Zhang (eds.), *Biosurveillance: Methods and Case Studies*, pp. 215–238. Chapman and Hall/CRC.

Höhle M, Meyer S, Paul M (2015). **surveillance**: *Temporal and Spatio-Temporal Modeling and Monitoring of Epidemic Phenomena*. R package version 1.10-0, URL `http://surveillance.r-forge.r-project.org/`.

Höhle M, Paul M, Held L (2009). "Statistical Approaches to the Monitoring and Surveillance of Infectious Diseases for Veterinary Public Health." *Preventive Veterinary Medicine*, **91**(1), 2–10. `doi:10.1016/j.prevetmed.2009.05.017`.

Ihaka R, Murrell P, Hornik K, Fisher JC, Zeileis A (2015). **colorspace**: *Color Space Manipulation*. R package version 1.2-6, URL `http://CRAN.R-project.org/package=colorspace`.

Johnson A (2015). **polyclip**: *Polygon Clipping*. R package version 1.3-2, ported to R by Adrian Baddeley and Brian Ripley, URL http://CRAN.R-project.org/package=polyclip.

Johnson SD (2010). "A Brief History of the Analysis of Crime Concentration." *European Journal of Applied Mathematics*, **21**(Special Double Issue 4-5), 349–370. ISSN 1469-4425. doi:10.1017/S0956792510000082.

Jombart T, Cori A, Didelot X, Cauchemez S, Fraser C, Ferguson N (2014). "Bayesian Reconstruction of Disease Outbreaks by Combining Epidemiologic and Genomic Data." *PLOS Computational Biology*, **10**(1), e1003457. doi:10.1371/journal.pcbi.1003457.

Keeling MJ, Rohani P (2008). *Modeling Infectious Diseases in Humans and Animals*. Princeton University Press. ISBN 0-691-11617-2. URL http://www.modelinginfectiousdiseases.org/.

Kermack WO, McKendrick AG (1927). "A Contribution to the Mathematical Theory of Epidemics." *Proceedings of the Royal Society of London A*, **115**(772), 700–721. doi:10.1098/rspa.1927.0118.

Lawson AB, Leimich P (2000). "Approaches to the Space-Time Modelling of Infectious Disease Behaviour." *IMA Journal of Mathematics Applied in Medicine and Biology*, **17**(1), 1–13.

Liboschik T, Fokianos K, Fried R (2015). "**tscount**: An R package for analysis of count time series following generalized linear models." *SFB 823 Discussion Paper 6/2015*, TU Dortmund. URL http://CRAN.R-project.org/package=tscount.

Malesios C, Demiris N, Kalogeropoulos K, Ntzoufras I (2014). "Bayesian Spatio-Temporal Epidemic Models with Applications to Sheep Pox." http://arxiv.org/abs/1403.1783.

Martinussen T, Scheike TH (2002). "A Flexible Additive Multiplicative Hazard Model." *Biometrika*, **89**(2), 283–298. ISSN 0006-3444. doi:10.1093/biomet/89.2.283.

Merl D, Johnson LR, Gramacy RB, Mangel M (2010). "**amei**: An R Package for the Adaptive Management of Epidemiological Interventions." *Journal of Statistical Software*, **36**(6), 1–32. ISSN 1548-7660. URL http://www.jstatsoft.org/v36/i06.

Meyer S (2015). **polyCub**: *Cubature over Polygonal Domains*. R package version 0.5-2, URL http://CRAN.R-project.org/package=polyCub.

Meyer S, Elias J, Höhle M (2012). "A Space-Time Conditional Intensity Model for Invasive Meningococcal Disease Occurrence." *Biometrics*, **68**(2), 607–616. doi:10.1111/j.1541-0420.2011.01684.x. http://arxiv.org/abs/1508.05740.

Meyer S, Held L (2014a). "Power-Law Models for Infectious Disease Spread." *The Annals of Applied Statistics*, **8**(3), 1612–1639. doi:10.1214/14-AOAS743.

Meyer S, Held L (2014b). "Supplement B of 'Power-Law Models for Infectious Disease Spread'." doi:10.1214/14-AOAS743SUPPB. http://www.biostat.uzh.ch/research/manuscripts/powerlaw.html.

Meyer S, Warnke I, Rössler W, Held L (2015). "Model-based testing for space-time interaction using point processes: An application to psychiatric hospital admissions in an urban area." Submitted to *Spatial and Spatio-temporal Epidemiology*.

Mohler GO, Short MB, Brantingham PJ, Schoenberg FP, Tita GE (2011). "Self-exciting Point Process Modeling of Crime." *Journal of the American Statistical Association*, **106**(493), 100–108. doi:10.1198/jasa.2011.ap09546.

Mossong J, Hens N, Jit M, Beutels P, Auranen K, Mikolajczyk R, Massari M, Salmaso S, Tomba GS, Wallinga J, Heijne J, Sadkowska-Todys M, Rosinska M, Edmunds WJ (2008). "Social Contacts and Mixing Patterns Relevant to the Spread of Infectious Diseases." *PLoS Medicine*, **5**(3), e74. doi:10.1371/journal.pmed.0050074.

Neal PJ, Roberts GO (2004). "Statistical Inference and Model Selection for the 1861 Hagelloch Measles Epidemic." *Biostatistics*, **5**(2), 249–261. doi:10.1093/biostatistics/5.2.249.

Obadia T, Haneef R, Boelle PY (2012). "The **R0** Package: A Toolbox to Estimate Reproduction Numbers for Epidemic Outbreaks." *BMC Medical Informatics and Decision Making*, **12**(147). ISSN 1472-6947. doi:10.1186/1472-6947-12-147.

Ogata Y (1988). "Statistical Models for Earthquake Occurrences and Residual Analysis for Point Processes." *Journal of the American Statistical Association*, **83**(401), 9–27. URL http://www.jstor.org/stable/2288914.

Ogata Y (1999). "Seismicity Analysis Through Point-process Modeling: A Review." *Pure and Applied Geophysics*, **155**(2), 471–507. ISSN 0033-4553. doi:10.1007/s000240050275.

Paul M, Held L (2011). "Predictive Assessment of a Non-Linear Random Effects Model for Multivariate Time Series of Infectious Disease Counts." *Statistics in Medicine*, **30**(10), 1118–1136. doi:10.1002/sim.4177.

Paul M, Held L, Toschke A (2008). "Multivariate Modelling of Infectious Disease Surveillance Data." *Statistics in Medicine*, **27**(29), 6250–6267. doi:10.1002/sim.3440.

Pebesma E (2012). "**spacetime**: Spatio-Temporal Data in R." *Journal of Statistical Software*, **51**(7), 1–30. URL http://www.jstatsoft.org/v51/i07/.

Pebesma E (2015). "CRAN Task View: Handling and Analyzing Spatio-Temporal Data." http://CRAN.R-project.org/web/views/SpatioTemporal.html. Version 2015-09-01.

Pebesma EJ, Bivand RS (2005). "Classes and methods for spatial data in R." *R News*, **5**(2), 9–13. URL http://CRAN.R-project.org/doc/Rnews/.

R Core Team (2015). *R: A Language and Environment for Statistical Computing*. R Foundation for Statistical Computing, Vienna, Austria. URL https://www.R-project.org/.

Rowlingson B, Diggle P (2015). **splancs**: *Spatial and Space-Time Point Pattern Analysis*. R package version 2.01-38, URL http://CRAN.R-project.org/package=splancs.

Ryan JA, Ulrich JM (2014). **xts**: *eXtensible Time Series*. R package version 0.9-7, URL http://CRAN.R-project.org/package=xts.

Salmon M, Schumacher D, Höhle M (2015). "Monitoring Count Time Series in R: Aberration Detection in Public Health Surveillance." *Journal of Statistical Software*. In press, http://arxiv.org/abs/1411.1292.

Sarkar D (2008). *Lattice: Multivariate Data Visualization with R.* Springer, New York. ISBN 978-0-387-75968-5, URL http://lmdvr.r-forge.r-project.org.

Scheike TH, Martinussen T (2006). *Dynamic Regression models for survival data.* Springer, NY.

Scheike TH, Zhang MJ (2011). "Analyzing Competing Risk Data Using the R **timereg** package." *Journal of Statistical Software*, **38**(2), 1–15. URL http://www.jstatsoft.org/v38/i02.

Schrödle B, Held L, Rue H (2012). "Assessing the Impact of a Movement Network on the Spatiotemporal Spread of Infectious Diseases." *Biometrics*, **68**(3), 736–744. doi:10.1111/j.1541-0420.2011.01717.x.

Silvapulle MJ, Sen PK (2005). *Constrained Statistical Inference: Order, Inequality, and Shape Constraints.* Wiley Series in Probability and Statistics. John Wiley & Sons. ISBN 0-471-20827-2.

Sommariva A, Vianello M (2007). "Product Gauss Cubature over Polygons based on Green's Integration Formula." *Bit Numerical Mathematics*, **47**(2), 441–453. ISSN 0006-3835. doi:10.1007/s10543-007-0131-2.

Stadler T, Bonhoeffer S (2013). "Uncovering Epidemiological Dynamics in Heterogeneous Host Populations Using Phylogenetic Methods." *Philosophical Transactions of the Royal Society of London B: Biological Sciences*, **368**(1614), 20120198. doi:10.1098/rstb.2012.0198.

Therneau TM (2015). *A Package for Survival Analysis in S.* Version 2.38, URL http://CRAN.R-project.org/package=survival.

Turlach BA (2013). **quadprog**: *Functions to solve Quadratic Programming Problems.* R package version 1.5-5, ported to R by Andreas Weingessel, URL http://CRAN.R-project.org/package=quadprog.

Utsu T, Ogata Y, Matsu'ura RS (1995). "The Centenary of the Omori Formula for a Decay Law of Aftershock Activity." *Journal of Physics of the Earth*, **43**(1), 1–33. doi:10.4294/jpe1952.43.1.

Venables WN, Ripley BD (2002). *Modern Applied Statistics with S.* Fourth edition. Springer, New York. ISBN 0-387-95457-0, URL http://www.stats.ox.ac.uk/pub/MASS4.

Vrbik I, Deardon R, Feng Z, Gardner A, Braun J (2012). "Using Individual-level Models for Infectious Disease Spread to Model Spatio-temporal Combustion Dynamics." *Bayesian Analysis*, **7**(3), 615–638. doi:10.1214/12-BA721.

Waller LA, Gotway CA (2004). *Applied Spatial Statistics for Public Health Data.* Wiley Series in Probability and Statistics. John Wiley & Sons. ISBN 0-471-66267-4. doi:10.1002/0471662682.

Wei W, Held L (2014). "Calibration Tests for Count Data." *TEST*, **23**(4), 787–805. doi:10.1007/s11749-014-0380-8.

Wickham H (2014). **memoise***: Memoise functions.* R package version 0.2.1, URL `http://CRAN.R-project.org/package=memoise`.

Wickham H (2015). **scales***: Scale Functions for Visualization.* R package version 0.3.0, URL `http://CRAN.R-project.org/package=scales`.

Xia Y, Bjørnstad ON, Grenfell BT (2004). "Measles Metapopulation Dynamics: A Gravity Model for Epidemiological Coupling and Dynamics." *The American Naturalist*, **164**(2), 267–281. ISSN 0003-0147. URL `http://www.jstor.org/stable/10.1086/422341`.

Xie Y (2013). "**animation**: An R Package for Creating Animations and Demonstrating Statistical Methods." *Journal of Statistical Software*, **53**(1), 1–27. URL `http://www.jstatsoft.org/v53/i01/`.

Xie Y (2015). *Dynamic Documents with R and **knitr***. The R Series, 2nd edition. Chapman and Hall/CRC, Boca Raton, Florida. ISBN 1-4987-1696-2. URL `http://yihui.name/knitr/`.

Affiliation:

Sebastian Meyer
Epidemiology, Biostatistics and Prevention Institute
University of Zurich
Hirschengraben 84
CH-8001 Zurich, Switzerland
E-mail: `sebastian.meyer@uzh.ch`
URL: `http://www.ebpi.uzh.ch/en/aboutus/departments/biostatistics.html`

Leonhard Held
Epidemiology, Biostatistics and Prevention Institute
University of Zurich
E-mail: `leonhard.held@uzh.ch`

Michael Höhle
Department of Mathematics
Stockholm University
E-mail: `hoehle@math.su.se`
URL: `http://www.math.su.se/~hoehle`